

Review

Permeability of Buccal Mucosa

Apipa Wanasathop , Priya B Patel, Hyojin A. Choi and S. Kevin Li * 

Division of Pharmaceutical Sciences, College of Pharmacy, University of Cincinnati, 231 Albert Sabin Way, MSB # 3005, Cincinnati, OH 45267, USA; wanasaaa@mail.uc.edu (A.W.); patel5pi@mail.uc.edu (P.B.P.); choih4@mail.uc.edu (H.A.C.)

* Correspondence: kevin.li@uc.edu; Tel.: +1-(513)-558-0977; Fax: +1-(513)-558-3233

Abstract: The buccal mucosa provides an alternative route of drug delivery that can be more beneficial compared to other administration routes. Although numerous studies and reviews have been published on buccal drug delivery, an extensive review of the permeability data is not available. Understanding the buccal mucosa barrier could provide insights into the approaches to effective drug delivery and optimization of dosage forms. This paper provides a review on the permeability of the buccal mucosa. The intrinsic permeability coefficients of porcine buccal mucosa were collected. Large variability was observed among the published permeability data. The permeability coefficients were then analyzed using a model involving parallel lipoidal and polar transport pathways. For the lipoidal pathway, a correlation was observed between the permeability coefficients and permeant octanol/water partition coefficients (K_{ow}) and molecular weight (MW) in a subset of the permeability data under specific conditions. The permeability analysis suggested that the buccal permeation barrier was less lipophilic than octanol. For the polar pathway and macromolecules, a correlation was observed between the permeability coefficients and permeant MW. The hindered transport analysis suggested an effective pore radius of 1.5 to 3 nm for the buccal membrane barrier.

Keywords: permeability; buccal; membrane; drug delivery; transport



Citation: Wanasathop, A.; Patel, P.B.; Choi, H.A.; Li, S.K. Permeability of Buccal Mucosa. *Pharmaceutics* **2021**, *13*, 1814. <https://doi.org/10.3390/pharmaceutics13111814>

Academic Editor: Barbara Luppì

Received: 24 September 2021

Accepted: 23 October 2021

Published: 31 October 2021

Publisher's Note: MDPI stays neutral with regard to jurisdictional claims in published maps and institutional affiliations.



Copyright: © 2021 by the authors. Licensee MDPI, Basel, Switzerland. This article is an open access article distributed under the terms and conditions of the Creative Commons Attribution (CC BY) license (<https://creativecommons.org/licenses/by/4.0/>).

1. Introduction

For effective drug delivery across a biological membrane, it is important to understand the transport behavior of the membrane for the drugs. The mechanisms of drug permeation across a biological membrane can be divided into passive, facilitated, and active transport. The effects of the metabolic barrier due to enzyme degradation and drug clearance from the tissue due to blood circulation and the lymphatic system can also be important. For example, effective drug clearance after tissue penetration is beneficial to systemic drug delivery but has a negative impact on local drug delivery. In general, the barrier property of a membrane due to passive transport can be described by its permeability coefficient.

Previous reviews have covered a variety of topics in buccal drug delivery. These review papers, which span the last several decades, include general overviews and updates of buccal drug delivery and its assessments [1–7], drug products utilizing this route of administration [8,9], and technologies to improve drug delivery via the buccal mucosa such as penetration enhancers, microadhesives, nanoparticles, and biopolymers [10–18]. In addition, buccal delivery of specific drugs and their clinical uses have been reviewed [19–22]. Review papers are also available on the topics of buccal delivery of macromolecules such as peptides, oligonucleotides, and vaccines [7,23–26]. Consequently, these topics are not the focus of the present review paper.

For the permeability of buccal mucosa, previous studies have analyzed the relationships between the permeability coefficients and physicochemical properties of drugs [27,28]. The effect of temperature and activation energy of membrane permeation were also investigated to understand the transport mechanism of buccal mucosa [29]. However, a comprehensive summary of buccal permeability data is not available in the literature.

The present paper provides a review on the permeability of the buccal mucosa for drug delivery. Porcine buccal mucosa has been the most common tissue in buccal drug delivery studies and was the focus of this review. The permeability coefficients of the buccal mucosa without the influence of formulations or the use of penetration enhancers (i.e., membrane intrinsic permeability) were summarized in this paper. The effects of lipophilicity and molecular weight of the permeants on their penetration across the buccal mucosa were examined. Analyses were performed to provide insights into a possible quantitative structure permeability relationship of passive transport across the buccal membrane that could be valuable in future drug delivery development.

2. Buccal Mucosa and Drug Delivery

Before the examination of buccal membrane permeability, this section provides a brief review of the buccal mucosa and buccal drug delivery. The oral mucosa is a complex series of tissues lining the oral cavity. It consists of tissue layers such as stratified squamous epithelium, basement membrane, and supporting connective tissues underneath. The buccal mucosa, in addition to the sublingual and gingival mucosa, is part of the oral mucosa. It is the area inside the cheek and between the gums and lower lips with an average surface area of $\sim 100 \text{ cm}^2$ [30]. The buccal mucosa consists of the outer epithelium and basement membrane. The non-keratinized stratified squamous epithelium forms the outer buccal epithelium. It is composed of mostly phospholipids and also proteins in the form of tonofilament. The basal layer of the epithelium differentiates into replacement cells that are shed from the outermost buccal surface. The epithelium, due to its morphology and lipid structure, is considered as the major barrier for the penetration of most drugs in buccal delivery. The basement membrane is a continuous layer of extracellular material and generally not considered as the major barrier for drug delivery. After the drug penetrates the buccal epithelium, it enters the systemic circulation via the vascularized tissue and jugular vein.

Buccal drug administration provides an alternative route for systemic drug delivery. It has several advantages over the gastrointestinal (GI) route by bypassing the hepatic first-pass effect, avoiding interference from acidity and enzymes relative to the GI tract, providing ease of dosing with the accessibility of the oral cavity and ease of drug removal in the event of adverse reactions. There are a number of commercial buccal drug delivery dosage forms in the market such as buccal tablet, spray, mucoadhesive, sublingual lozenge, chewing gum, film, and oromucosal solution. The disadvantages of buccal drug delivery include the (a) barrier of the buccal mucosa that its permeability may be too low for certain drugs, (b) interference of saliva that can dilute the drug for absorption, and (c) variable environment in the oral cavity due to food consumption and other daily activities. For example, although the permeability of the buccal mucosa is generally higher than that of the stratum corneum [31], it is generally lower than that of the GI mucosal monolayer [32,33], as can be seen by comparing their values to the buccal permeabilities presented later in the present review. To overcome this barrier, chemical penetration enhancers such as surfactants, physical penetration enhancers such as iontophoresis, and formulation technologies such as mucoadhesive and polymeric dosage forms can be utilized for buccal drug delivery. In order to fully utilize these enhancement methods and to develop effective buccal drug delivery systems, it is important to understand the intrinsic passive permeability of the buccal mucosa.

3. Permeability of Buccal Mucosa and Data Variability

The permeants and their buccal permeability coefficients collected for this review are listed in Table A1 (see Appendix A). The permeability coefficients were obtained from the references [27–29,34–107] and the logarithmic values of the permeability coefficients in cm/s ($\log P$) were calculated. Only permeability data from porcine buccal mucosa were collected for the analysis because the majority of previous permeation studies was with the porcine tissue. In addition, a comparison between the porcine tissue and tissues from

other species (bovine, canine, hamster, monkey, and human) showed that their permeability coefficients were within similar orders of magnitudes except for hamster tissue that displayed higher permeability (Table 1). In some cases, engineered tissues (TR146 tissue model, EpiOral tissue model, and Caco-2 cells) also showed higher permeability than the porcine buccal tissue. It should be noted that the data shown in Table 1 are not intended to be comprehensive but to support the use of porcine buccal permeability data in the analyses of the present review. In the data collection, another selection criterion was unperturbed buccal membrane. Only buccal permeability coefficients (intrinsic permeability) without formulation influences and organic solvent manipulations were considered. Results obtained at temperatures outside the normal range of 34–37 °C were not included. For the model analyses, the physicochemical properties of the permeants such as pKa, octanol/water partition coefficient (K_{ow}), and octanol/water distribution coefficient (D_{ow}), when available, were also collected from the previous studies (Table A1). D_{ow} , which is the ratio of the concentration of unionized species in the octanol phase to the concentration of both ionized and unionized species in the aqueous phase, is related to K_{ow} as described by Equation (A2) (see Appendix B). When the pKa, K_{ow} , or D_{ow} values were not available in the references, the pKa and K_{ow} values were obtained from PubChem [108] and D_{ow} was calculated using the pKa and pH of the permeant solutions in the studies (see Equations (A3) and (A4)).

Table 1. Comparison between the permeability coefficients of porcine buccal tissue and other species and engineered tissues. Data are shown as log P (P in cm/s).

Permeant	Porcine ^a	Bovine	Canine	Hamster	Monkey	Human	Engineered Tissue	Ref ^b
Acebutolol	−7.40, −7.57						−5.46 ^d	[34]
Alprenolol	−5.70						−4.47 ^d	[34]
Atenolol	−7.55 to −6.72						−6.41 ^e , −5.68 ^d	[34,39]
Caffeine	−5.57 to −4.63			−2.21			−4.96 ^e , −6.11 ^f	[39,109,110]
Cathine	−5.50						−5.00 ^e	[39]
Cathinone	−5.52						−4.92 ^e	[39]
Estradiol	−4.54, −4.29		−4.88					[111]
Fentanyl	−5.15		−4.54					[112]
Galantamine	−4.93						−4.70 ^d	[68]
Insulin	−8.18						−5.92 ^d , −7.10 ^d	[70,113]
Labetalol	−7.70, −6.26						−5.11 ^d	[34]
Lidocaine	−6.57 to −4.77			−2.13				[109]
Mannitol	−7.00 to −5.60				−6.51	−6.62, −6.62	−5.39 ^d , −5.66 ^d	[34,78,114]
Metoprolol	−8.60 to −4.97					−5.10	−4.47 ^d	[34,78]
Morphine	−5.88, −5.72	−6.60						[84]
Naltrexone	−5.28, −4.76						−5.07 ^{c,f} , −4.98 ^d	[86,115]
Nicotine	−7.90 to −4.50					−3.77 ^c		[116]
Norephedrine	−5.67						−5.01 ^e	[39]
Oxprenolol	−6.05, −5.52						−4.40 ^d	[34]
Pindolol	−6.92, −6.70						−4.51 ^d	[34]
Propranolol	−5.89 to −4.85						−5.38 ^d	[34]
Tertatolol	−6.00						−4.57 ^d	[34]
Testosterone	−5.96				−4.72	−5.74	−4.70 ^d	[34]
Timolol	−6.52						−4.62 ^d	[34]
Verapamil	−4.60			−2.52				[109]
Water	−5.09, −4.94		−4.29		−5.77, −4.62	−6.02	−4.28 ^d	[34,111,117,118]

^a Permeability value from Table A1. ^b References listed are for buccal tissues from other species and engineered tissues. References for porcine buccal tissue are listed in Table A1. ^c Multiple permeability values are available in the reference and the average value of log P was used. ^d TR146 cell culture model. ^e Caco-2 cell model. ^f EpiOral model.

When permeability data of the same permeants are available from buccal permeation studies performed by multiple research groups under similar experimental conditions, large variability was observed between the data generated among these research groups. To compare the permeability data in these studies (from different research groups), the average of the mean permeability coefficients presented in these studies was determined for the permeant and the coefficient of variation (CV) was calculated (CV = ratio of the standard

deviation to the average $\times 100\%$). The CV of the permeability coefficients was then plotted against the average permeability coefficient of each permeant (Figure 1). Although the high CV from the $n = 2$ studies can be related to the nature that only two studies were compared, most permeants have CV much higher than 50% even without considering the variability of the $n = 2$ studies. This is significantly higher than the CV generally encountered in diffusion cell permeation experiments [119]. Possible causes of the large variability could be the (a) different sources of porcine tissues (age, species), (b) different methods of tissue preparation and the resulting tissue conditions, and (c) different experimental conditions among these studies. For comparison, the average and CV of the mean permeability coefficients from studies of the same groups (from different permeation studies such as different papers published by the same research group) were also calculated and the CV was plotted against the average permeability coefficient of each permeant in the figure. The CV values from the same research groups are generally smaller than those from different research groups (open symbols vs. closed symbols, respectively). Furthermore, there is no apparent relationship between the variabilities and permeability coefficients of the permeants in both comparisons (of the same and different research groups), indicating that the variabilities were likely not transport-mechanism related. The large variabilities observed among the permeability data of the same permeants from the studies published by different research groups suggested the potential difficulty in using the literature permeability data to determine the quantitative structure permeability relationship for buccal drug delivery.

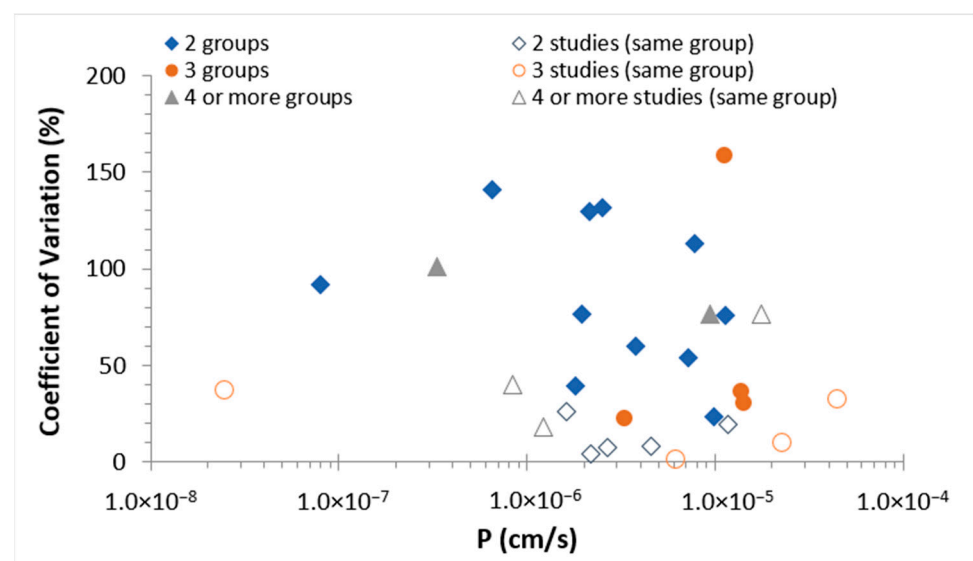


Figure 1. Assessment of permeation data variability. CV of the permeability data among different research groups were plotted against the average of the permeability data. In this case, CV was calculated using the reported mean values of the same permeant from different studies conducted by different research groups and plotted as a data point using the average of these values. CV of the data among different studies from the same research groups were also determined for comparison. In this case, CV was calculated using the reported mean values of the same permeant from different studies conducted by the same research group. Permeants in studies from different research groups are: antipyrine, atenolol, bupivacaine, buspirone, caffeine, didanosine, dideoxycytidine, estradiol, mannitol, metoprolol (2 data sets of different conditions), naltrexone, ondansetron, oxprenolol, propranolol (2 data sets of different conditions), and triamcinolone acetamide. Symbols: permeant data from two (closed diamonds), three (closed circles), and four or more (closed triangles) research groups. Permeants in studies from the same research groups are: acyclovir, antipyrine, caffeine, decitabine, diazepam, didanosine, estradiol, mannitol, morphine, nicotine (2 data sets of different conditions), triamcinolone acetamide. Symbols: permeant data from two (open diamonds), three (open circles), and four or more (open triangles) studies from the same research groups.

For the permeability analyses in the present review, when the permeability data were from different studies of the same research group, the average value of the permeability coefficients published in these studies was calculated and used as an individual data point. When the permeability data were from different research groups, the result from each research group was treated as an individual data point in the analyses; these data were analyzed as separate data points with the same weighing factor as if they were different permeants.

4. Membrane Transport Theory

In order to examine the relationships between the permeability coefficients of buccal mucosa and the physicochemical properties of the permeants, this section provides a brief review of transport theory for drug permeation across biological membranes. In general, the permeability of a biological membrane can be described by a parallel pathway permeation model of lipoidal and polar pathways [120,121]. The lipoidal pathway (or transcellular pathway) describes the permeation across the lipid barrier from the membrane lipid lamella structure, and the polar pathway (or pore pathway) describes the permeation across the aqueous channels across the membrane via the paracellular route or membrane defects. For the permeation of a weak acid or weak base, which is pH dependent, the flux of the permeant and its permeability coefficient can be expressed as [32]:

$$J = J_u + J_i = (P_u C_u + P_i C_i) = (P_u f_u + P_i (1 - f_u)) C \quad (1)$$

$$P = (P_l + P_p) f_u + P_p (1 - f_u) = P_l f_u + P_p \quad (2)$$

where J is flux, P is permeability coefficient of the membrane, C is concentration, f_u is the fraction of unionized permeant, subscripts u and i represent the unionized and ionized permeants, and subscripts l and p represent the lipoidal and polar pathways, respectively. Assuming that the microenvironment of the lipid lamellae in the membrane can be mimicked by octanol and the contribution of P_p is minimal, and using the relationship between membrane diffusion coefficient and permeant molecular weight [31], the permeability coefficient can be expressed as (see derivation of Equation (A10) in Appendix B):

$$\log P = \log D_{ow} + c MW + constant \quad (3)$$

where MW is permeant molecular weight, c is the coefficient of MW , and $constant$ is a constant. For permeants that are not affected by pH, $D_{ow} = K_{ow}$ and Equation (3) becomes:

$$\log P = \log K_{ow} + c MW + constant \quad (4)$$

Equations (3) and (4) were the models used in the analyses of the buccal permeability data (see Section 5).

When the microenvironment of the lipid barrier is different from that of octanol, membrane partitioning can be described by the linear free energy relationship [122]:

$$\log K_m = a \log K_{ow} + \log b. \quad (5)$$

where K_m is membrane partition coefficient and a and b are constants. The slope of the $\log P$ vs. $\log K_{ow}$ relationship (or $\log P$ vs. $\log D_{ow}$ for the permeants that are pH dependent due to ionization) indicates the lipophilicity of the rate limiting barrier for permeation across the membrane. Replacing K_{ow} in the derivation of Equation (3) by this free energy relationship, Equation (4) can be rewritten as (see the derivation of Equation (A13) in Appendix B):

$$\log(P/D_{ow}) = (a - 1) \log K_{ow} + c MW + constant \quad (6)$$

In addition to Equations (3) and (4), the buccal permeability data were also analyzed by Equation (6) (see Section 5).

For permeation across the polar pathway in a biological membrane, which can be modeled as aqueous channels with hindered transport, the permeability coefficient of the polar pathway (P_p) can be described by the polar pathway transport model [123,124].

$$P_p = \varepsilon K_p H D_{aq} / h_m'' \quad (7)$$

where ε is membrane porosity, K_p is the partition coefficient due to permeant-to-membrane interactions, D_{aq} is aqueous diffusion coefficient, H is hindered transport factor for diffusion, and h_m'' is the effective thickness of the membrane for the polar pathway. The hindered transport factor is a function of the permeant molecular size and the pore size of the polar pathway [125].

$$H = 6\pi(1 - \lambda)^2 / \left[2.25\pi^2\sqrt{2}(1 - \lambda)^{-2.5} \left(1 + \sum_{n=1}^2 a_n(1 - \lambda)^n \right) + \sum_0^4 a_{n+3}\lambda^n \right] \quad (8)$$

where λ is the ratio of permeant radius to pore radius, $a_1 = -1.21667$, $a_2 = 1.53359$, $a_3 = -22.5083$, $a_4 = -5.6117$, $a_5 = -0.3363$, $a_6 = -1.216$, and $a_7 = 1.647$. When $\lambda < 0.4$, Equation (8) is equivalent to the commonly used Renkin equation. The hindered transport model can be used to characterize the effective size of a pore transport pathway [126–128]. Assuming that the effects due to permeant-to-membrane interactions in the aqueous transport pathway are small (i.e., $K_p \approx 1$), the ratio of the permeability coefficients of two permeants is related to the ratio of hindered transport factors of the permeants.

$$(P_{p,1}/D_{aq,1}) / (P_{p,2}/D_{aq,2}) = H_1/H_2 \quad (9)$$

where subscripts 1 and 2 represent permeant 1 and permeant 2, respectively. By fitting Equation (9) with the permeability ratio data, the effective pore radius of the polar pathway can be evaluated (see Section 6).

5. Effects of Lipophilicity and Molecular Weight on the Permeation of Small Molecules

Figure 2 shows the relationship between the permeability coefficients of buccal mucosa and the lipophilicities of the permeants in Table A1, in which the lipophilicities are measured by K_{ow} . The correlation between $\log P$ and $\log K_{ow}$ was poor. By taking into account the fraction of ionization of the permeants, Figure 3 shows the relationship between the permeability coefficients and D_{ow} of the permeants. The correlation between the permeability coefficients and lipophilicities of the permeants improved when D_{ow} (instead of K_{ow}) was used (Figure 3 vs. Figure 2), but the correlation was still relatively poor.

Figure 4 shows the relationship between the permeability coefficients of buccal mucosa and the MW of the permeants. There was no direct correlation between the permeability coefficients and MW of the permeants without the consideration of their lipophilicities. The effect of permeant MW on membrane permeability was then investigated by regression analyses (MS Excel Linest function) using $\log D_{ow}$ and MW as two independent variables. Three parameters (a , c , and *constant*) were fitted to the experimental data using a similar relationship as Equation (3):

$$\log P = a \log D_{ow} + c \text{ MW} + \text{constant} \quad (10)$$

Table 2 presents the result of this analysis. The incorporation of MW in the permeability analysis did not have any significant effects on the correlation between $\log P$ and $\log D_{ow}$ for the quantitative structure permeability relationship.

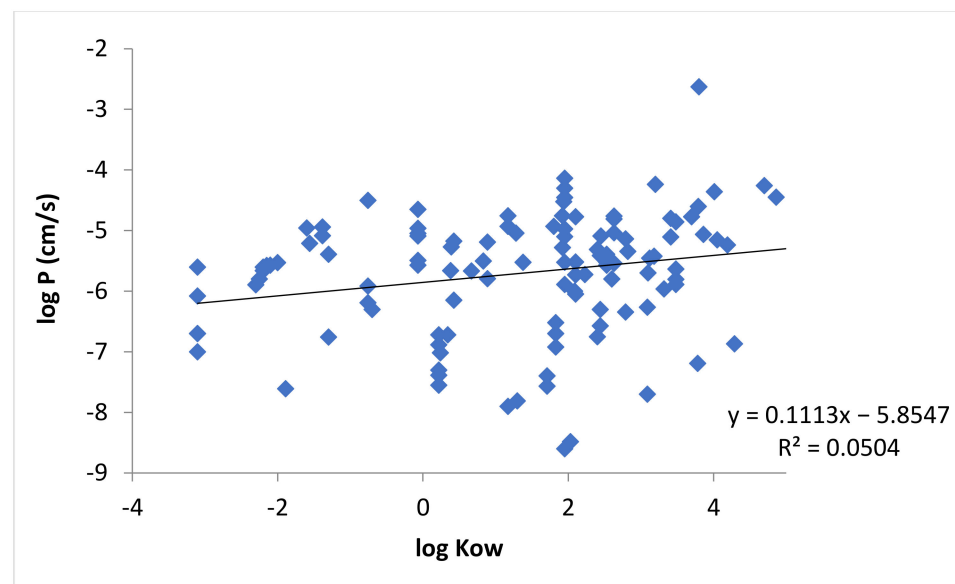


Figure 2. Relationship between $\log P$ and $\log K_{ow}$ for all applicable permeants in Table A1.

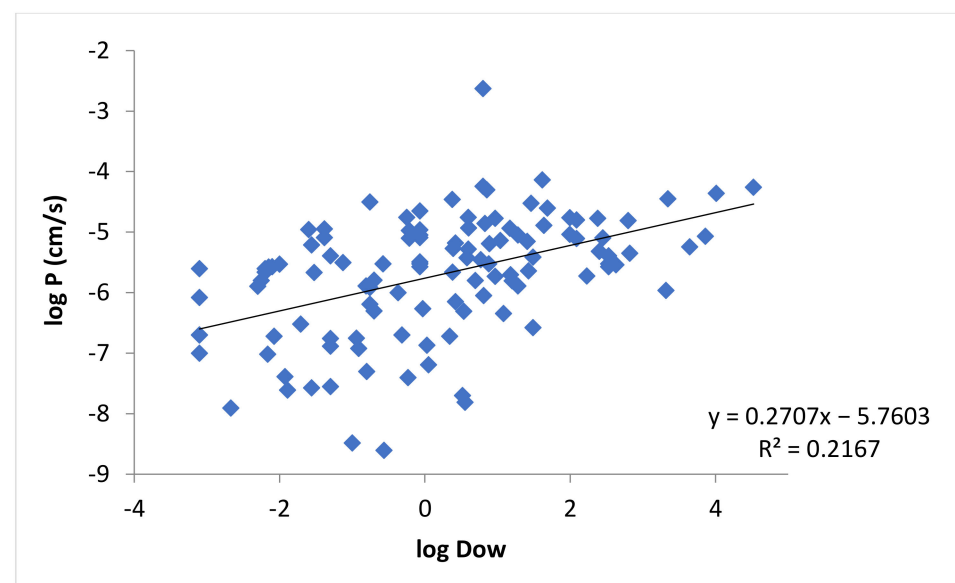
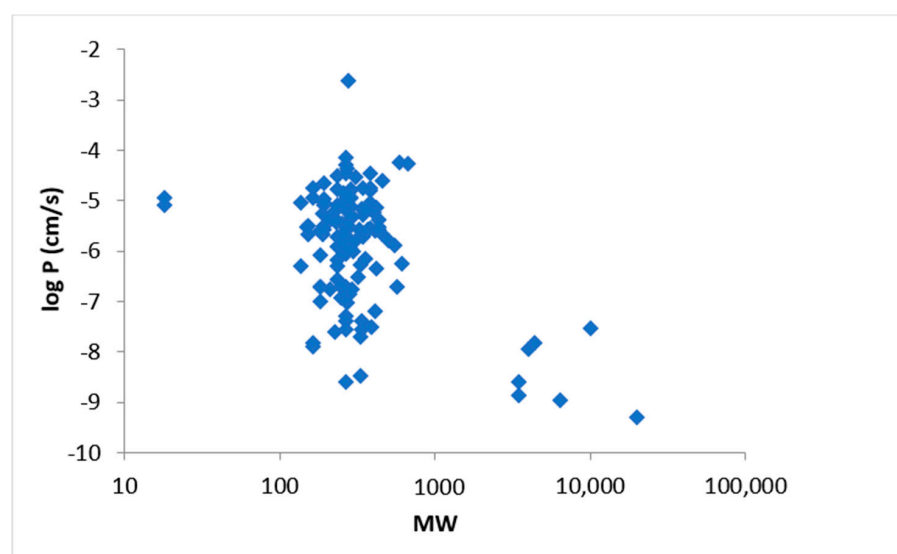


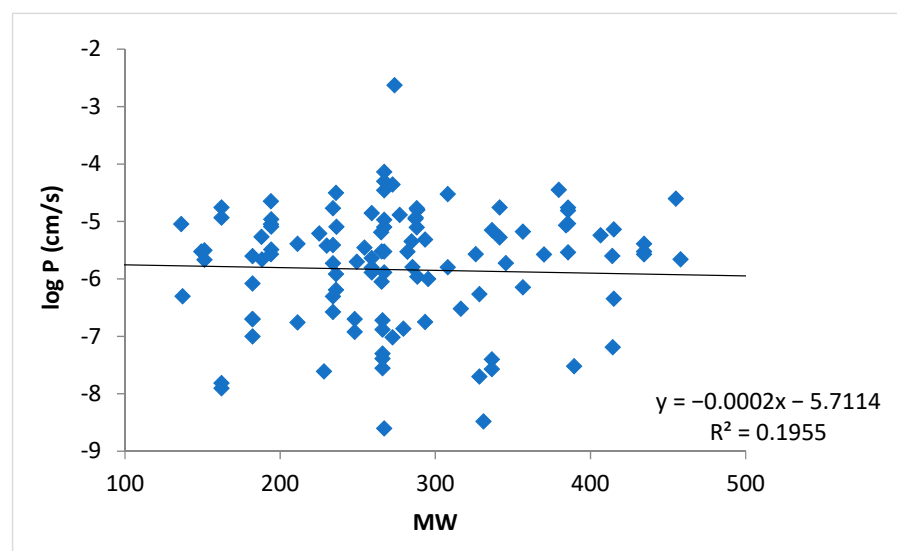
Figure 3. Relationship between $\log P$ and $\log D_{ow}$ for all applicable permeants in Table A1.

Table 2. Regression analysis results of $\log P$ with $\log D_{ow}$ and MW as independent variables (first three rows) and $\log (P/D_{ow})$ with $\log K_{ow}$ and MW as independent variables (last three rows), using the data of all permeants and then permeants with $\log D_{ow} > -1$ and > 0 . The parameters are defined in Equations (6) and (10). The values presented are the least squares means and standard errors of the parameters.

Condition	a	c	constant	R^2
$\log P$ vs. $\log D_{ow}$ and MW ; all data; $n = 115$	0.29 ± 0.05	-0.0008 ± 0.0009	-5.5 ± 0.3	0.222
$\log P$ vs. $\log D_{ow}$ and MW ; $\log D_{ow} > -1$; $n = 88$	0.37 ± 0.08	-0.0021 ± 0.0011	-5.3 ± 0.3	0.183
$\log P$ vs. $\log D_{ow}$ and MW ; $\log D_{ow} > 0$; $n = 62$	0.22 ± 0.10	-0.0007 ± 0.0011	-5.4 ± 0.3	0.072
$\log (P/D_{ow})$ vs. $\log K_{ow}$ and MW ; all data; $n = 115$	0.44 ± 0.05	-0.0014 ± 0.0009	-4.8 ± 0.3	0.588
$\log (P/D_{ow})$ vs. $\log K_{ow}$ and MW ; $\log D_{ow} > -1$; $n = 88$	0.60 ± 0.09	-0.0031 ± 0.0013	-4.7 ± 0.3	0.382
$\log (P/D_{ow})$ vs. $\log K_{ow}$ and MW ; $\log D_{ow} > 0$; $n = 62$	0.64 ± 0.12	-0.0027 ± 0.0014	-5.0 ± 0.4	0.279



(a)



(b)

Figure 4. (a) Relationship between $\log P$ and MW for all applicable permeants in Table A1. (b) Enlarged figure to evaluate the relationship between $\log P$ and MW of permeants in the 130–460 Dalton range.

Equation (10) was derived under the assumption of minimal contribution from the polar pathway to the total permeability of the buccal membrane (i.e., $P_p \ll P$; see the assumption in Equation (A8) in Appendix B). For example, permeants that have low D_{ow} (e.g., $D_{ow} < -1$) could predominantly utilize the polar pathway for buccal membrane permeation and have low or comparable permeability coefficients to those of the polar pathway, so the inclusion of these data in the analysis can introduce errors. To this end, $\log D_{ow} < -1$ was applied as an exclusion criterion in the evaluation of the “ $\log P$ vs. $\log D_{ow}$ and MW ” relationship; only the permeability data of permeants with $\log D_{ow} > -1$ and water were analyzed. Water was not excluded in the analyses because it could readily permeate lipid bilayers without using the polar pathway. The exclusion of these data did not improve the “ $\log P$ vs. $\log D_{ow}$ and MW ” correlation and further exclusion of the permeants that have $D_{ow} < 0$ also did not show any improvement (Table 2). To account for possible differences between K_m and K_{ow} , additional analyses were performed using Equation (6) and the permeability data. The results are presented in Table 2. The approach

of $\log(P/D_{ow})$ vs. $\log K_{ow}$ and MW provided better correlations than those of the “ $\log P$ vs. $\log D_{ow}$ and MW ” when compared using the same permeability datasets (first row vs. fourth row, second row vs. fifth row, and third row vs. sixth row in Table 2). However, except for the dataset of “all data” (fourth row in Table 2), the correlations were still relatively poor. The improvement in correlations using the model of Equation (6) is consistent with the conclusion that the buccal membrane barrier is less lipophilic than octanol (K_m vs. K_{ow} ; see discussion later in this section and Section 7). For the correlation using all data, the quantitative structure permeability relationship observed was: $\log(P/D_{ow}) = -0.56 \log K_{ow} - 0.0014 MW - 4.8$ (with $R^2 = 0.588$).

Membrane transport of weak acid and weak base can be affected by a number of factors including the fraction of permeant ionization that is a function of permeant pKa and solution pH (i.e., pH dependent permeant charges). Due to this uncertainty, permeant transport that is pH dependent and is related to the fraction of permeant ionization can introduce errors in the permeability analyses. Figure 5 shows the relationship between the permeability coefficients and K_{ow} by excluding the permeants with ionization as a function of pH (i.e., using only pH independent permeants) in the analysis. The exclusion of the pH dependent permeants slightly improved the correlation of the relationship between $\log P$ and $\log K_{ow}$ (compared to Figure 2).

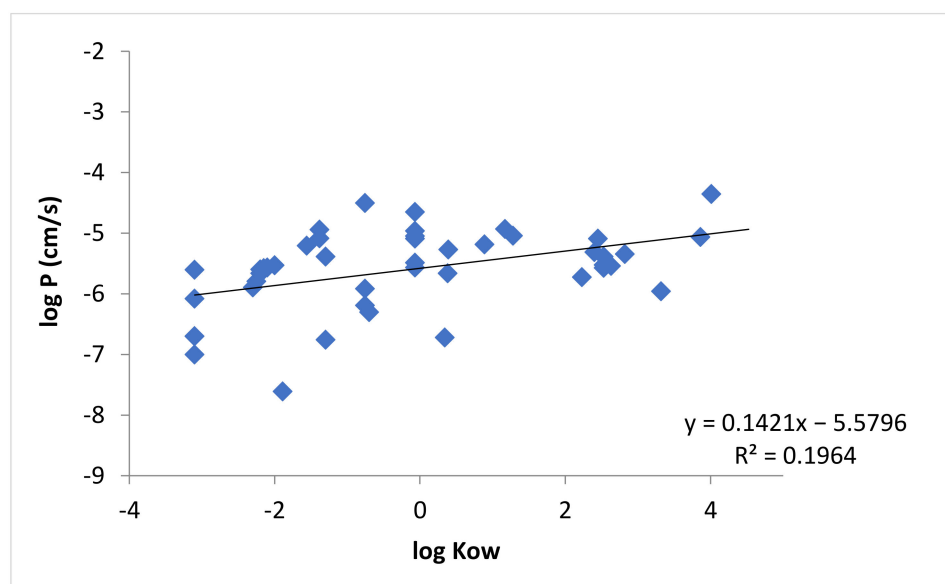


Figure 5. Relationship between $\log P$ and $\log K_{ow}$ for permeants that are not affected by pH ionization (pH independent permeants) in Table A1.

With the pH independent permeants as the dataset, regression analyses were performed using $\log K_{ow}$ and MW as two independent variables, a , c , and $constant$ as the parameters, and a similar relationship as Equation (4):

$$\log P = a \log K_{ow} + c MW + constant \quad (11)$$

The incorporation of MW in the analysis improved the correlation (Table 3). To consider the influence of the polar pathway (P_p), the exclusion criteria of $\log K_{ow} < -1$ and < 0 were applied to the analyses of these permeants. The exclusion of the permeants that have $\log K_{ow} < -1$ provided a better correlation of the “ $\log P$ vs. $\log K_{ow}$ and MW ” relationship. Increasing the $\log K_{ow}$ value in the exclusion criterion to analyze only permeants with $\log K_{ow} > 0$ further improved the “ $\log P$ vs. $\log K_{ow}$ and MW ” correlation ($R^2 = 0.615$). The results of these analyses are summarized in Table 3.

Table 3. Regression analysis results of $\log P$ with $\log K_{ow}$ and MW as independent variables, using the data of pH independent permeants and then with the conditions of $\log K_{ow} > -1$ and >0 . The parameters are defined in Equation (11). The values presented are the least squares means and standard errors of the parameters.

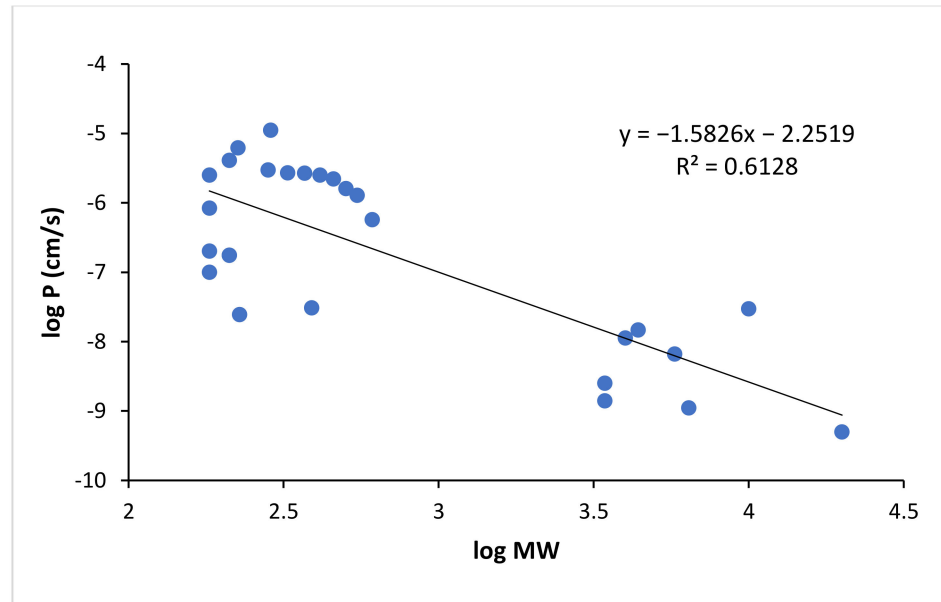
Condition	a	c	constant	R^2
$\log P$ vs. $\log K_{ow}$ and MW ; all data; $n = 44$	0.16 ± 0.04	-0.0012 ± 0.0007	-5.2 ± 0.2	0.246
$\log P$ vs. $\log K_{ow}$ and MW ; $\log K_{ow} > -1$; $n = 28$	0.17 ± 0.07	-0.0031 ± 0.0009	-4.8 ± 0.2	0.325
$\log P$ vs. $\log K_{ow}$ and MW ; $\log K_{ow} > 0$; $n = 18$	0.20 ± 0.06	-0.0033 ± 0.0006	-4.8 ± 0.2	0.615

An interesting observation in the present study is the slopes of $\log P$ vs. $\log K_{ow}$ (or $\log P$ vs. $\log D_{ow}$) in the permeability, lipophilicity, and MW correlation analyses. These slopes (coefficient a) are significantly smaller than unity for the linear free energy relationship between membrane partitioning and octanol/water partitioning (K_m vs. K_{ow} , Equation (5)), and this can be attributed to a number of factors. First, the transport rate-limiting barrier of the buccal mucosa can be less lipophilic compared to octanol. This can lead to a slope significantly smaller than unity in the linear free energy relationship between water-to-membrane and water-to-octanol partitioning for buccal membrane permeation. Second, the influences of the polar pathway and underlying tissues of the buccal tissues can create lower and upper boundaries, respectively, for the buccal permeability range to accurately determine the slope (coefficient a) in the linear free energy relationship. When the permeability range is narrow in the permeability vs. lipophilicity relationship, the data points at the boundaries or outside this range can “skew” the data, resulting in an apparent slope less than the actual value in the “ $\log P$ vs. $\log K_{ow}$ and MW ” (or “ $\log P$ vs. $\log D_{ow}$ and MW ”) correlation. Although employing the exclusion criteria of $\log K_{ow}$ (or $\log D_{ow}$) < -1 and < 0 could minimize the impact of the polar pathway and reduce this “skewing” effect in the data analysis, as shown in the improvement of the correlations in Table 3, the use of these exclusion criteria might not be sufficient. For example, there was no improvement in the correlation after applying the $\log D_{ow} < -1$ and < 0 exclusion criteria in the correlations in Table 2. Third, the variability of the permeability data in the previous studies and the uncertainties of $\log D_{ow}$ can affect the correlations. Particularly, the general improvement of the “ $\log P$ vs. $\log K_{ow}$ and MW ” correlations with the pH independent permeants (i.e., without changes in ionization such as fraction of ionization due to pH) over the correlations of “ $\log P$ vs. $\log D_{ow}$ and MW ” (first three rows in Table 2 vs. Table 3) can be attributed to the decrease in uncertainties related to permeant ionization due to pH. Previous studies have suggested the possibility of membrane pH that is different from solution pH surrounding the biological membrane (e.g., skin, GI) [129–131], and this type of phenomena can lead to errors in calculating the fraction of ionization for buccal membrane permeation in the analyses. Regardless of these influencing factors and uncertainties in the present permeability analyses, the results indicate apparent correlation slopes of buccal membrane permeation vs. $\log K_{ow}$ that are significantly smaller than those of other biological membranes such as lipid bilayers (~2.0–2.8), skin (~0.7–0.8), and cornea (~0.5) [31,122,132], except when the model of Equation (6) was used. In addition, there is a lack of molecular size (or MW) dependence for the permeation of small molecules across the lipoidal barrier of the buccal membrane, which may be “masked” by data variability, when all the data were included in the analyses. When the exclusion criteria were applied to the permeants to take into account the model limitations and the uncertainties in permeant pH-ionization and partitioning, a reasonable quantitative structure permeability relationship was observed: $\log P = 0.2 \log K_{ow} - 0.0033 MW - 4.8$ (with $R^2 = 0.615$, Table 3 last row).

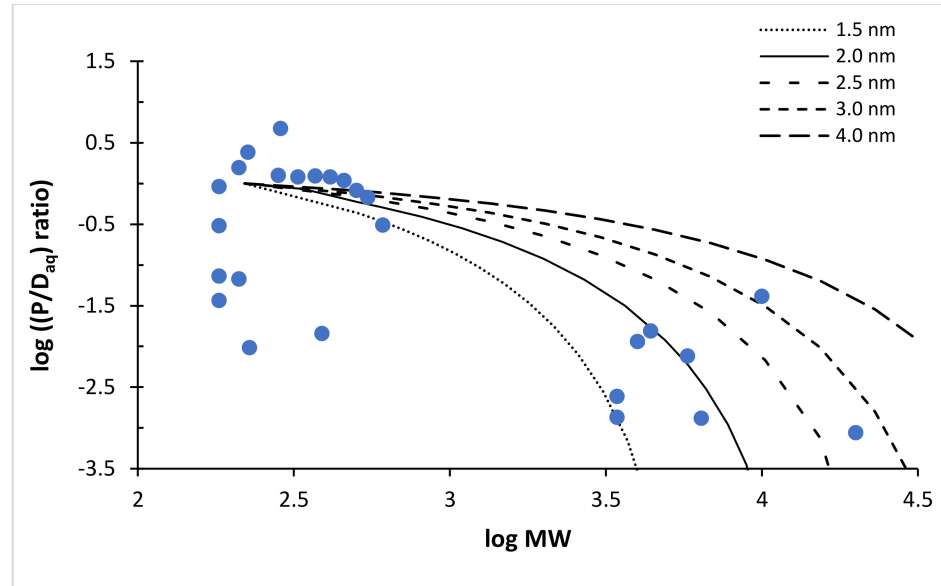
6. Effective Pore Size for the Permeation of Macromolecules

The permeation of macromolecules across a biological membrane is anticipated to be through the paracellular route of the membrane. This transport pathway can be modeled by the polar pathway and hindered transport theory (Equations (7) and (8)). Figure 6a presents the relationship between the permeability coefficients and MW of the macromolecules and

the polar permeants that have $\log K_{ow} < -1$ and are not pH dependent (i.e., not weak acid or weak base) for the buccal mucosa. With the inclusion of the macromolecules in the permeability analysis, unlike the analysis of only small permeants, a steep size dependence of permeability was observed with a linear regression slope of -1.58 and $R^2 = 0.613$ for the $\log P$ vs. $\log MW$ relationship.



(a)



(b)

Figure 6. (a) Relationship between $\log P$ and $\log MW$ of polar permeants (pH independent and $\log K_{ow} < -1$) and macromolecules from Table A1. (b) Comparison of the $\log (P/D_{aq})$ ratio and $\log H$ ratio vs. $\log MW$ of the polar permeants and macromolecules. The reference P/D_{aq} and H values in (b) are those of a hypothetical small permeant with permeability coefficient and MW equivalent to the average values of the permeants with MW < 300 Dalton in (a). Symbols: experimental P/D_{aq} ratio data. Lines: H ratios calculated with pore radius of 1.5 nm (dotted), 2 nm (solid), 2.5 nm (dash-dot), 3 nm (short dashes), and 4 nm (dashes) using Equation (8).

To examine the effective pore size of the polar pathway, the ratios of the permeability and diffusion coefficients were calculated and compared to a reference (Equation (9)). The reference point in this analysis (Permeant 2 in Equation (9)) was a hypothetical small permeant with an average permeability coefficient and MW of the small permeants that have MW < 300 Dalton in Figure 6a. Figure 6b shows the relationship between the P/D_{aq} ratio and MW from the permeability data and the H ratio calculated using Equation (8), based on the reference point. The theoretical hindered transport relationship of molecular size and pore size shows a significant decrease in the H ratio when the molecular size increases from 300 to 20,000 Dalton and the pore size (radius) decreases from 4 nm to 1.5 nm. By comparing the theoretical hindered transport H ratios and the experimental P/D_{aq} ratios, the result suggests an effective pore radius in the range of 1.5 to 3 nm for the buccal polar pathway (or paracellular pathway). The result in this analysis is in agreement with that in a previous study that investigated the polar pathway using a polymer of different molecular sizes (polyethylene glycol) [96]. In addition, the effective pore size of the buccal mucosa was in the same order of magnitude as other biological membranes such as skin, cornea, conjunctiva, nail, and GI mucosal monolayer [124,126,133,134].

7. Permeability Analysis Discussion and Consideration

The present review examined the permeability of porcine buccal mucosa and the major findings are as follows. Large variability of the permeability data was observed in previous studies from different research groups even when the permeability measurements were performed under similar experimental conditions (Figure 1). In general, the correlation between buccal membrane permeability and permeant lipophilicity was relatively poor (Figure 2) and no general permeability-to-MW relationship was observed (Figure 4) when either permeant lipophilicity (as indicated by K_{ow}) or MW was used as the single independent variable in the analyses of the permeability data for all permeants.

To further investigate the relationship between permeant lipophilicity and the permeability of the lipoidal pathway in the buccal mucosa, the permeability was described better by $\log D_{ow}$ than $\log K_{ow}$ (Figure 3 vs. Figure 2) consistent with the transport theory of uncharged permeants due to pH dependent ionization of the permeants (i.e., weak acid and weak base) when all permeants were used in the analyses. However, the correlation between $\log P$ and $\log D_{ow}$ was still relatively poor with no improvement in the correlation when permeant MW was incorporated as an additional independent variable in the analyses; there was no observable effect of permeant MW on the permeability. To take into account the contribution of the polar pathway (P_p) to membrane permeability, the permeability data were also evaluated by allowing only permeants with $\log D_{ow} > -1$ or > 0 in the analyses. These exclusion criteria did not improve the correlations of the “ $\log P$ vs. $\log D_{ow}$ and MW” relationship for the permeants studied (Table 2). A hypothesis of the poor correlations is data variability and errors related to the fraction of ionization calculations (e.g., membrane pH different from solution pH and errors introduced in the calculations of $\log D_{ow}$). The data were therefore analyzed using only pH independent permeants (permeants without fraction of ionization as a function of pH).

For the pH independent permeants, a better correlation was observed in the $\log P$ vs. $\log K_{ow}$ relationship (Figure 5 vs. Figure 2). The correlation improved with the incorporation of MW as an additional independent variable and further improvement was observed with the exclusion of the permeants that likely utilize the polar pathway, i.e., by limiting the analyses to only permeants with $\log K_{ow} > -1$ and > 0 (Table 3). When these exclusion criteria were applied, a reasonable quantitative structure permeability relationship of “ $\log P$ vs. $\log K_{ow}$ and MW” was observed ($R^2 = 0.615$). Another observation in the analyses is the coefficient of $\log K_{ow}$ in the “ $\log P$ vs. $\log K_{ow}$ and MW” relationship (coefficient a in Equation (11)). This coefficient denotes the slope of the linear free energy relationship between K_m and K_{ow} (see Equation (5)). The slope of 0.2 is smaller than those observed with other biological membranes and suggests that the barrier domain of buccal membrane permeation is less lipophilic than octanol.

In the investigation of the relationship between permeant MW and the permeability of the polar pathway in the buccal mucosa using the macromolecules and pH independent permeants that have $\log K_{ow} < -1$, a correlation between $\log P$ and MW was observed. The result of the hindered transport analysis suggests an effective pore radius of 1.5 to 3 nm in the buccal mucosa for the permeation of polar permeants and macromolecules. This pore size value is in the same order of magnitude as other biological membranes such as skin, cornea, conjunctiva, nail, and GI mucosal monolayer.

It should be pointed out that the present review is focused on porcine buccal mucosa because (a) the majority of the permeability data in previous studies were from this animal model and (b) the similarity between human and porcine buccal mucosae. In addition, the permeability data presented in this review can be different from the permeability for drug delivery in practice because drug formulations usually contain excipients that can enhance membrane permeability for more effective drug delivery and this review is focused only on the intrinsic permeability of the buccal mucosa. The conclusion from the analyses (model of Equation (10)) using all the permeant data collected in this review is affected by (a) data variabilities in the previous studies (i.e., variabilities of P , K_{ow} , and D_{ow}), (b) model limitations such as the influence of the polar pathway and the difference between K_m and K_{ow} , and (c) uncertainties in permeant pH-ionization relationship (i.e., the use of D_{ow}) arise from undefined membrane pH that can be different from the solution pH. The model of Equation (6) could account for the difference between K_m and K_{ow} but not the other factors. Hence, there was a need to apply certain exclusion criteria in the analyses, leading to a smaller dataset, in order to generate meaningful results. Although a more comprehensive analysis of buccal permeability could not be completed in the present review due to the availability and variability of the data in the literature, the results provide insights into possible quantitative structure permeability relationships of the buccal mucosa.

8. Conclusions

The buccal mucosa provides a number of advantages as an alternative route of drug administration. To develop more effective buccal drug delivery systems, knowledge on the intrinsic permeability of the buccal mucosa is essential. However, an extensive review of the permeability data is not available despite the numerous studies and reviews on the topic of buccal drug delivery. In the present review, the intrinsic permeability coefficients of porcine buccal mucosa were collected, a database of the permeability coefficients was generated, and the influences of permeant lipophilicity (as $\log K_{ow}$ and $\log D_{ow}$) and molecular size (as MW) on the permeability of the buccal mucosa were analyzed. The first observation was the large variability among the published permeability data (of the same permeants). Such variability in buccal permeability studies in the literature could lead to poor correlation (coefficient of determination) in analyzing the permeability data for a possible quantitative structure permeability relationship. In the analyses of all permeability data including the permeants with pH dependent ionization, the permeability was described better by $\log D_{ow}$ than $\log K_{ow}$ for membrane partitioning and permeation, but the correlation was relatively poor with no observable effect of permeant MW. This can be attributed to the difference between solution and membrane pH when using the fraction of unionized permeant in the solution to account for membrane permeation. For the permeability data of pH independent permeants (which are not affected by ionization due to pH in the analysis), a better correlation was observed and the correlation improved with the incorporation of MW as the additional independent variable. The analysis of the relationship between the permeability and partition coefficient of the permeants for the buccal membrane barrier suggested an apparent linear free energy relationship that was less lipophilic than octanol. For the permeability data of macromolecules and polar permeants, an effective pore radius of 1.5 to 3 nm was found for the buccal mucosa using the hindered transport theory. The results obtained in this review could improve our understanding of the buccal mucosal barrier and assist in the development of more effective buccal drug delivery and dosage forms.

Author Contributions: Conceptualization, S.K.L.; Methodology, S.K.L.; Formal Analysis, A.W., S.K.L.; Investigation, A.W., H.A.C., P.B.P., S.K.L.; Resources, S.K.L.; Data Curation, A.W., H.A.C., P.B.P., S.K.L.; Writing—Original Draft Preparation, S.K.L.; Writing—Review & Editing, A.W., H.A.C., P.B.P., S.K.L.; Visualization, S.K.L.; Supervision, S.K.L.; Project Administration, S.K.L.; Funding Acquisition, S.K.L. All authors have read and agreed to the published version of the manuscript.

Funding: The research in this publication was supported in part by National Institute of Dental & Craniofacial Research (NIDCR) of the National Institutes of Health (NIH) under Award Number R15 DE028701. The content is solely the responsibility of the authors and does not necessarily represent the official views of the NIH.

Institutional Review Board Statement: Not applicable.

Informed Consent Statement: Not applicable.

Data Availability Statement: Not applicable.

Acknowledgments: The authors thank Michael Murawsky for his inputs.

Conflicts of Interest: The authors have no conflicts of interest.

Appendix A. Permeability Data of Porcine Buccal Mucosa

Table A1. Properties of permeants (MW, log K_{ow} , and pKa), permeability coefficients, and sources of buccal permeation data.

Permeant	MW	log K_{ow}	pKa	pH	log D_{ow}	log P (cm/s)	Ref
Acebutolol	336.4	1.71	9.46	6.8	−1.56	−7.57	[28]
Acebutolol	336.4	1.71	9.46	7.4	−0.23	−7.40	[34]
Acyclovir	225.2	−1.56	2.52, 9.35	6.8	−1.56	−5.21	[35]
Acyclovir	225.2	−1.56	2.52, 9.35	3.3–8.8	−1.56	−5.20 ^d	[36]
Alprenolol	249.4	3.1	9.5	7.4	1.18	−5.70	[34]
Amitriptyline	277.4	5.04	9.31	6.8	1.64	−4.89	[27]
Antipyrine	188.2	0.39	1.45	6.8	0.39	−5.65	[37]
Antipyrine	188.2	0.39	1.45	6.8	0.39	−5.27	[27]
Antipyrine	188.2	0.38	1.4	6.8	0.38	−5.67	[29]
Atenolol	266.3	0.22	9.54	7.4	−0.80	−7.30	[34]
Atenolol	266.3	0.22	9.54	7.4	−1.92	−7.39	[38]
Atenolol	266.3	0.22	9.54	6.8	−1.30	−7.55	[27]
Atenolol	266.3	0.22	9.54	6.8	−1.30	−6.88	[28]
Atenolol	266.3	0.22	9.54	7.25	−2.07	−6.72	[39]
Atenolol ^a	266.3	0.22	9.54	6.8	— ^c	— ^a	[40]
Benznidazole ^a	260.2	0.91	— ^c	— ^c	0.91	— ^a	[41]
Bupivacaine	288.4	3.41	8.1	6.8	2.09	−5.10	[37]
Bupivacaine	288.4	3.7	8.1	6.8	2.38	−4.77	[27]
Bupivacaine	288.4	3.41	8.1	6.8	2.09	−4.80	[29]
Buspirone	385.5	2.63	4.12, 7.32	varying pH unionized form data	2.63	−5.54	[42]
Buspirone	385.5	2.63	4.12, 7.32	6.8	2.00	−5.04	[37]
Buspirone	385.5	2.63	4.12, 7.32	6.8	2.80	−4.81	[27]
Buspirone	385.5	2.63	4.12, 7.32	6.8	2.00	−4.76	[29]
Caffeine	194.2	−0.07	10.4	6.8	−0.07	−5.05	[27]
Caffeine	194.2	−0.07	10.4	— ^c	−0.07	−4.70	[43]
Caffeine	194.2	−0.07	10.4	6.8	−0.07	−5.49	[37]
Caffeine	194.2	−0.07	10.4	— ^c	−0.07	−4.63 ^d	[44]
Caffeine	194.2	−0.07	10.4	6.8	−0.07	−5.09	[29]
Caffeine	194.2	−0.07	10.4	6.8	−0.07	−4.96	[45]
Caffeine	194.2	−0.07	10.4	7.25	−0.07	−5.57	[39]
Carbamazepine	236.3	2.45	13.9	6.75	2.45	−5.09	[46]
Carprofen	273.7	3.8	4.4	7.4	0.80	−2.63	[47]
Carvedilol ^a	406.5	4.19	7.8	7.4	3.64	— ^a	[48]
Carvedilol	406.5	4.19	7.8	7.4	3.64	−5.24	[49]
Carvedilol ^a	406.5	4.19	7.8	7.4	3.64	— ^a	[50]
Cathine	151.2	0.83	9.2	7.25	−1.12	−5.50	[39]
Cathinone	149.2	1.38	9.2	7.25	−0.57	−5.52	[39]
Decitabine	228.2	−1.89	— ^c	7.0	−1.89	−7.64 ^d	[51]
Diazepam	284.7	2.82	3.4	6.8	2.82	−5.37	[52]
Diazepam	284.7	2.82	3.4	6.8	2.82	−5.32	[45]
Didanosine	236.2	−0.754	9.13	7.4	−0.754	−5.92 ^d	[53]

Table A1. Cont.

Permeant	MW	log K_{ow}	pKa	pH	log D_{ow}	log P (cm/s)	Ref
Didanosine	236.2	-0.754	9.13	7.4	-0.754	-4.50	[54]
Didanosine	236.2	-0.754	9.13	7.4	-0.754	-6.19	[55]
Dideoxycytidine	211.2	-1.3	— ^c	7.1	-1.3	-5.39	[56]
Dideoxycytidine	211.2	-1.3	— ^c	7.4	-1.3	-6.76	[57]
Diltiazem	414.5	2.79	7.7	6.8	1.04	-5.14	[27]
Diltiazem	414.5	2.79	7.7	6.0	1.08	-6.34	[58]
Donepezil	379.5	4.86	8.9	7.4	3.35	-4.45	[59]
Doxepin	279.4	4.29	8.96	4.7	0.03	-6.87	[60]
Endomorphin-1	610.7	— ^c	— ^c	7.1	— ^c	-6.25	[61]
Estradiol	272.4	4.01	— ^c	7.4	4.01	-4.29 ^d	[44]
Estradiol	272.4	4.01	— ^c	7.4	4.01	-4.54	[43]
Estradiol ^a	272.4	4.01	— ^c	7.4	4.01	— ^a	[62]
Felodipine	384.2	3.86	5.07	7.4	3.86	-5.06	[63]
Fentanyl	336.5	4.05	9	7.0	1.41	-5.15	[64]
FITC (fluorescein isothiocyanate)	389.4	— ^c	— ^c	— ^c	— ^c	-7.52	[65]
FITC-dextran	4000	— ^c	— ^c	— ^c	— ^c	-7.95	[65]
FITC-dextran	4400	— ^c	— ^c	6.4	— ^c	-7.83	[66]
FITC-dextran	10,000	— ^c	— ^c	— ^c	— ^c	-7.53	[65]
FITC-dextran	20,000	— ^c	— ^c	— ^c	— ^c	<-9.3 ^e	[65]
FITC-dextran	40,000	— ^c	— ^c	— ^c	— ^c	<-9.3 ^e	[65]
Flecainide	414.3	3.78	9.3	7.4	0.05	-7.19	[67]
Furosemide	330.7	2.03	4.7	6.8	-1.00	-8.48	[27]
Galantamine	287.35	1.8	7.97	6.8	0.60	-4.93	[68]
Hydrocortisone acetate ^a	404.5	2.19	— ^c	— ^c	2.19	— ^a	[69]
Insulin	5778	— ^c	— ^c	7.4	— ^c	-8.18	[70]
Irinotecan CPT-11	586.7	3.2	9.3	7.4	0.80	-4.24	[71]
Isoniazid	137.1	-0.7	1.8	6.8	— ^c	-6.30	[72]
Ketoprofen	254.3	3.12	4.45	7.4	— ^c	-5.45	[73]
Labetalol	328.4	3.09	9.3	7.4	0.52	-7.70	[34]
Labetalol	328.4	3.09	9.3	6.8	-0.03	-6.26	[28]
Lamotrigine	265.1	0.89	5.7	7.4	0.89	-5.19	[74]
Lidocaine	234.3	2.1	7.9	6.8	0.97	-4.77	[27]
Lidocaine	234.3	2.44	7.9	6.0	0.53	-6.30	[58]
Lidocaine	234.3	2.44	7.9	7.0	1.49	-6.57	[75]
Lidocaine ^a	234.3	2.44	7.9	7.0	— ^c	— ^a	[76]
Lidocaine	234.3	2.1	7.9	7.4	0.97	-5.73	[73]
Lidocaine	234.3	2.44	7.9	7.0	1.49	-5.41	[77]
Mannitol	182.2	-3.1	— ^c	7.4	-3.1	-6.70	[34]
Mannitol	182.2	-3.1	— ^c	7.4	-3.1	-6.70	[78]
Mannitol	182.2	-3.1	— ^c	— ^c	-3.1	-5.60	[79]
Mannitol	182.2	-3.1	— ^c	6.8	-3.1	-6.08 ^d	[80]
Mannitol	182.2	-3.1	— ^c	7.4	-3.1	-7.00	[81]
Metoprolol	267.4	1.95	9.56	7.4	-0.07	-5.52	[34]
Metoprolol	267.4	1.95	9.56	7.4	-0.21	-4.97	[78]
Metoprolol	267.4	1.95	9.56	6.8	-0.81	-5.89	[27]
Metoprolol	267.4	1.95	9.56	6.8	-0.56	-8.60	[28]
Metoprolol	267.4	1.95	9.56	7.4, 8.0, 8.5, 9.5 ^f	-0.21	-5.10, -4.46, -4.30, -4.14 ^f	[82]
Morphine	285.3	0.89	8.21	6.8	-0.70	-5.72 ^d	[83]
Morphine	285.3	0.89	8.21	— ^c	-0.70	-5.88	[84]
Naltrexone	341.4	1.92	8.1	6.8	0.60	-4.76	[85]
Naltrexone	341.4	1.92	8.1	6.8	0.60	-5.28	[86]
Naproxen	230.3	3.18	4.2	6.8	0.58	-5.42	[27]
Nicotine	162.2	1.17	3.04, 7.84	varying pH unionized form data	1.17	-5.00	[87]
Nicotine	162.2	1.17	3.4, 8.2	unionized form data	1.17	-4.88	[88]
Nicotine	162.2	1.3	3.26, 8.06	7.4	0.55	-7.81	[89]
Nicotine	162.2	1.17	3.04, 7.84	4.0	-2.67	-7.90	[58]
Nicotine	162.2	1.17	3.4, 8.2	6.8	-0.25	-5.16	[52]
Nicotine	162.2	1.17	3.4, 8.2	6.8	-0.25	-5.26 ^d	[79]
Nicotine	162.2	1.17	3.4, 8.2	6.8	-0.25	-5.10	[90]
Nicotine	162.2	1.17	3.4, 8.2	6.8	-0.25	-4.50 ^d	[80]
Nimesulide	308.3	1.94	6.5	6.8	1.46	-4.52	[27]
Norephedrine	151.2	0.67	9.44	7.25	-1.52	-5.67	[39]
Oligonucleotide	6405	— ^c	— ^c	— ^c	— ^c	-8.96	[91]
Omeprazole	345.4	2.23	4.8	7.0	2.23	-5.73	[92]
Ondansetron	293.4	2.4	7.34	unionized form data	2.4	-5.31	[93]

Table A1. Cont.

Permeant	MW	log K_{ow}	pKa	pH	log D_{ow}	log P (cm/s)	Ref
Ondansetron	293.4	2.4	7.34	4.0	−0.94	−6.75	[94]
Oxprenolol	265.4	2.1	9.67	7.4	0.88	−5.52	[34]
Oxprenolol	265.4	2.1	9.67	6.8	0.81	−6.05	[28]
Pindolol	248.3	1.83	9.54	7.4	−0.31	−6.70	[34]
Pindolol	248.3	1.83	9.54	6.8	−0.91	−6.92	[27]
Pioglitazone	356.4	0.425	5.19	7.4	0.42	−5.18	[63]
Pioglitazone	356.4	0.425	5.19	— ^c	0.42	−6.15	[95]
Polyethylene glycol	282	−2	— ^c	7.4	−2.0	−5.53	[96]
Polyethylene glycol	326	−2.1	— ^c	7.4	−2.1	−5.57	[96]
Polyethylene glycol	370	−2.15	— ^c	7.4	−2.15	−5.58	[96]
Polyethylene glycol	414	−2.2	— ^c	7.4	−2.2	−5.60	[96]
Polyethylene glycol	458	−2.2	— ^c	7.4	−2.2	−5.66	[96]
Polyethylene glycol	502	−2.25	— ^c	7.4	−2.25	−5.80	[96]
Polyethylene glycol	546	−2.3	— ^c	7.4	−2.3	−5.89	[96]
Prilocaine ^a	220.3	2.11	7.89	7.4	— ^c	— ^a	[76]
Propranolol	259.3	3.48	9.45	7.4	1.28	−5.89	[34]
Propranolol	259.3	3.48	9.45	6.8	0.83	−4.85	[27]
Propranolol	259.3	3.48	9.45	6.8	1.20	−5.80	[28]
Propranolol	259.3	3.48	9.45	7.4	1.43	−5.64	[97]
Salbutamol ^a	239.3	1.4	10.3	7.1	−1.80	— ^a	[98]
Salmon calcitonin	3431.9	— ^c	— ^c	4.0	— ^c	−8.60	[99]
Salmon calcitonin	3431.9	— ^c	— ^c	7.4	— ^c	−8.86	[100]
Saquinavir	670.8	4.7	7.1	7.4	4.52	−4.26	[101]
Sotalol	272.4	0.24	9.8, 8.3	7.4	−2.16	−7.02	[67]
Steroidal glycoside P57 (extract) ^b	— ^c	— ^c	— ^c	7.0	— ^c	−4.66 ^b	[102]
Tacrine ^a	198.3	2.71	9.95	7.4	0.31	— ^a	[103]
Tenofovir	287.2	−1.6	— ^c	— ^c	−1.6	−4.95	[54]
Tertatolol	295.4	2.09	9.8	7.4	−0.37	−6.00	[34]
Testosterone	288.4	3.32	— ^c	7.4	3.32	−5.96	[34]
Tetramethylpyrazine	136.2	1.28	— ^c	— ^c	1.28	−5.04	[104]
Thiocolchicoside	563.6	0.34	— ^c	6.8	0.34	−6.72	[105]
Timolol	316.4	1.83	9.21	7.4	−1.71	−6.52	[34]
Triamcinolone acetonide	434.5	2.53	— ^c	7.4	2.53	−5.39	[106]
Triamcinolone acetonide	434.5	2.53	— ^c	— ^c	2.53	−5.55	[43]
Triamcinolone acetonide	434.5	2.53	— ^c	— ^c	2.53	−5.60	[107]
Triamcinolone acetonide	434.5	2.53	— ^c	6.75	2.53	−5.52	[46]
Verapamil	454.6	3.79	8.9	6.8	1.69	−4.60	[27]
Warfarin	308.3	2.6	4.9	6.8	0.69	−5.80	[27]
Water	18	−1.38	— ^c	7.4	−1.38	−5.09	[34]
Water	18	−1.38	— ^c	7.4	−1.38	−4.94	[81]

^a Permeability data with formulations involving organic solvents or enhancers in the permeation experiments. The data were not used in the present analysis. ^b Not sufficient information for use in the present analysis. ^c Not applicable or not available. ^d Multiple permeability values are available in the reference and the average value of log p was used. ^e Below detection limit. ^f Multiple pH conditions are available.

Appendix B. Derivation of Equations in Model Analyses

From Equation (2) in “Membrane Transport Theory” using a parallel pathway permeation model of lipoidal and polar pathways [120,121], the permeability coefficient of the membrane (P) can be expressed as [32]:

$$P = P_l f_u + P_p \quad (\text{A1})$$

where f_u is the fraction of unionized permeant and subscripts l and p represent the lipoidal and polar pathways, respectively. The fraction of unionized permeant is related to the octanol/water distribution coefficient (D_{ow}) and octanol/water partition coefficient (K_{ow}).

$$D_{ow} = K_{ow} f_u \quad (\text{A2})$$

$$\text{where } f_u = 1 / \left(1 + 10^{(pH - pKa)} \right) \text{ for weak acid} \quad (\text{A3})$$

$$\text{and } f_u = 1 / \left(1 + 10^{(pK_a - pH)} \right) \text{ for weak base} \quad (\text{A4})$$

Combining Equations (A1) and (A2),

$$P = P_l(D_{ow}/K_{ow}) + P_p \quad (\text{A5})$$

Assuming that the microenvironment of the lipid lamellae in the membrane can be mimicked by octanol, membrane partition coefficient can be estimated by K_{ow} (i.e., $K_m = K_{ow}$):

$$P_l = (K_m D_m / h_m) = (K_{ow} D_m / h_m) \quad (\text{A6})$$

where D_m is membrane diffusion coefficient, K_m is membrane partition coefficient, and h_m is effective thickness of the membrane. The relationship between the permeability of lipid membrane (e.g., lipid bilayer) and permeant lipophilicity defined by its K_{ow} in Equation (A6) is commonly used in membrane permeation model. Combining Equations (A5) and (A6),

$$P = (D_{ow} D_m / h_m) + P_p \quad (\text{A7})$$

When the contribution of P_p is minimal, Equation (A7) can be rewritten as:

$$\log P = \log D_{ow} + \log D_m + h_m' \quad (\text{A8})$$

where h_m' is a constant related to the effective thickness. The membrane diffusion coefficient can be expressed as [31]:

$$\log D_m = \log D_0 + c MW \quad (\text{A9})$$

where MW is permeant molecular weight, D_0 is the hypothetical diffusion coefficient of permeants with zero molecular volume, and c is a constant. Equation (A8) can be rewritten as:

$$\log P = \log D_{ow} + c MW + \text{constant} \quad (\text{A10})$$

where constant is a constant in the relationship. Or,

$$\log P = \log K_{ow} + c MW + \text{constant} \quad (\text{A11})$$

when $D_{ow} = K_{ow}$ for permeants that are not affected by pH.

A linear free energy relationship can be used to describe the microenvironment of the lipid barrier when it is different from that of octanol for membrane partitioning [122]:

$$K_m = b(K_{ow})^a \quad (\text{A12})$$

Replacing K_{ow} in Equation A6 by the relationship of Equation (A12) and rearranging the equation as in the derivation from Equations (A5)–(A10),

$$\log(P/D_{ow}) = (a - 1) \log K_{ow} + c MW + \text{constant} \quad (\text{A13})$$

References

- Hao, J.; Heng, P.W. Buccal delivery systems. *Drug Dev. Ind. Pharm.* **2003**, *29*, 821–832. [[CrossRef](#)] [[PubMed](#)]
- Birudaraj, R.; Mahalingam, R.; Li, X.; Jasti, B.R. Advances in buccal drug delivery. *Crit. Rev. Ther. Drug Carr. Syst.* **2005**, *22*, 295–330. [[CrossRef](#)]
- Pinto, S.; Pintado, M.E.; Sarmiento, B. In vivo, ex vivo and in vitro assessment of buccal permeation of drugs from delivery systems. *Expert Opin. Drug Deliv.* **2020**, *17*, 33–48. [[CrossRef](#)]
- Patel, V.F.; Liu, F.; Brown, M.B. Modeling the oral cavity: In vitro and in vivo evaluations of buccal drug delivery systems. *J. Control. Release* **2012**, *161*, 746–756. [[CrossRef](#)]
- Harris, D.; Robinson, J.R. Drug delivery via the mucous membranes of the oral cavity. *J. Pharm. Sci.* **1992**, *81*, 1–10. [[CrossRef](#)]
- Shojaei, A.H. Buccal mucosa as a route for systemic drug delivery: A review. *J. Pharm. Pharm. Sci.* **1998**, *1*, 15–30.
- Patel, V.F.; Liu, F.; Brown, M.B. Advances in oral transmucosal drug delivery. *J. Control. Release* **2011**, *153*, 106–116. [[CrossRef](#)]

8. Senel, S.; Rathbone, M.J.; Cansiz, M.; Pather, I. Recent developments in buccal and sublingual delivery systems. *Expert Opin. Drug Deliv.* **2012**, *9*, 615–628. [[CrossRef](#)] [[PubMed](#)]
9. Sattar, M.; Sayed, O.M.; Lane, M.E. Oral transmucosal drug delivery—current status and future prospects. *Int. J. Pharm.* **2014**, *471*, 498–506. [[CrossRef](#)] [[PubMed](#)]
10. Nicolazzo, J.A.; Reed, B.L.; Finnin, B.C. Buccal penetration enhancers—How do they really work? *J. Control. Release* **2005**, *105*, 1–15. [[CrossRef](#)] [[PubMed](#)]
11. Hassan, N.; Ahad, A.; Ali, M.; Ali, J. Chemical permeation enhancers for transbuccal drug delivery. *Expert Opin. Drug Deliv.* **2010**, *7*, 97–112. [[CrossRef](#)] [[PubMed](#)]
12. Laffleur, F. Mucoadhesive polymers for buccal drug delivery. *Drug Dev. Ind. Pharm.* **2014**, *40*, 591–598. [[CrossRef](#)] [[PubMed](#)]
13. Tran, P.H.L.; Duan, W.; Tran, T.T.D. Recent developments of nanoparticle-delivered dosage forms for buccal delivery. *Int. J. Pharm.* **2019**, *571*, 118697. [[CrossRef](#)] [[PubMed](#)]
14. Macedo, A.S.; Castro, P.M.; Roque, L.; Thome, N.G.; Reis, C.P.; Pintado, M.E.; Fonte, P. Novel and revisited approaches in nanoparticle systems for buccal drug delivery. *J. Control. Release* **2020**, *320*, 125–141. [[CrossRef](#)] [[PubMed](#)]
15. Singla, A.K.; Chawla, M.; Singh, A. Potential applications of carbomer in oral mucoadhesive controlled drug delivery system: A review. *Drug Dev. Ind. Pharm.* **2000**, *26*, 913–924. [[CrossRef](#)]
16. Salamat-Miller, N.; Chittchang, M.; Johnston, T.P. The use of mucoadhesive polymers in buccal drug delivery. *Adv. Drug Deliv. Rev.* **2005**, *57*, 1666–1691. [[CrossRef](#)]
17. Sudhakar, Y.; Kuotsu, K.; Bandyopadhyay, A.K. Buccal bioadhesive drug delivery—a promising option for orally less efficient drugs. *J. Control. Release* **2006**, *114*, 15–40. [[CrossRef](#)]
18. Wanasathop, A.; Li, S.K. Iontophoretic drug delivery in the oral cavity. *Pharmaceutics* **2018**, *10*, 121. [[CrossRef](#)] [[PubMed](#)]
19. Mystakidou, K.; Katsouda, E.; Parpa, E.; Vlahos, L.; Tsiatas, M.L. Oral transmucosal fentanyl citrate: Overview of pharmacological and clinical characteristics. *Drug Deliv.* **2006**, *13*, 269–276. [[CrossRef](#)] [[PubMed](#)]
20. Dinsmore, W.W.; Wyllie, M.G. The long-term efficacy and safety of a testosterone mucoadhesive buccal tablet in testosterone-deficient men. *BJU Int.* **2012**, *110*, 162–169. [[CrossRef](#)]
21. Garnock-Jones, K.P. Fentanyl buccal soluble film: A review in breakthrough cancer pain. *Clin. Drug Investig.* **2016**, *36*, 413–419. [[CrossRef](#)] [[PubMed](#)]
22. Pergolizzi, J.V., Jr.; Raffa, R.B.; Fleischer, C.; Zampogna, G.; Taylor, R., Jr. Management of moderate to severe chronic low back pain with buprenorphine buccal film using novel bioerodible mucoadhesive technology. *J. Pain Res.* **2016**, *9*, 909–916. [[CrossRef](#)]
23. Smart, J.D. Buccal drug delivery. *Expert Opin. Drug Deliv.* **2005**, *2*, 507–517. [[CrossRef](#)]
24. Kraan, H.; Vrieling, H.; Czerkinsky, C.; Jiskoot, W.; Kersten, G.; Amorij, J.P. Buccal and sublingual vaccine delivery. *J. Control. Release* **2014**, *190*, 580–592. [[CrossRef](#)]
25. Morales, J.O.; McConville, J.T. Novel strategies for the buccal delivery of macromolecules. *Drug Dev. Ind. Pharm.* **2014**, *40*, 579–590. [[CrossRef](#)] [[PubMed](#)]
26. Caon, T.; Jin, L.; Simoes, C.M.; Norton, R.S.; Nicolazzo, J.A. Enhancing the buccal mucosal delivery of peptide and protein therapeutics. *Pharm. Res.* **2015**, *32*, 1–21. [[CrossRef](#)] [[PubMed](#)]
27. Kokate, A.; Li, X.; Williams, P.J.; Singh, P.; Jasti, B.R. In silico prediction of drug permeability across buccal mucosa. *Pharm. Res.* **2009**, *26*, 1130–1139. [[CrossRef](#)]
28. Amores, S.; Lauroba, J.; Calpena, A.; Colom, H.; Gimeno, A.; Domenech, J. A comparative ex vivo drug permeation study of beta-blockers through porcine buccal mucosa. *Int. J. Pharm.* **2014**, *468*, 50–54. [[CrossRef](#)]
29. Kulkarni, U.D.; Mahalingam, R.; Li, X.; Pather, I.; Jasti, B. Effect of experimental temperature on the permeation of model diffusants across porcine buccal mucosa. *AAPS PharmSciTech* **2011**, *12*, 579–586. [[CrossRef](#)]
30. Gandhi, R.B.; Robinson, J.R. Oral cavity as a site for bioadhesive drug delivery. *Adv. Drug Deliv. Rev.* **1994**, *13*, 43–74. [[CrossRef](#)]
31. Potts, R.O.; Guy, R.H. Predicting skin permeability. *Pharm. Res.* **1992**, *9*, 663–669. [[CrossRef](#)] [[PubMed](#)]
32. Adson, A.; Burton, P.S.; Raub, T.J.; Barsuhn, C.L.; Audus, K.L.; Ho, N.F. Passive diffusion of weak organic electrolytes across Caco-2 cell monolayers: Uncoupling the contributions of hydrodynamic, transcellular, and paracellular barriers. *J. Pharm. Sci.* **1995**, *84*, 1197–1204. [[CrossRef](#)]
33. Tsutsumi, K.; Li, S.K.; Ghanem, A.H.; Ho, N.F.; Higuchi, W.I. A systematic examination of the in vitro Ussing chamber and the in situ single-pass perfusion model systems in rat ileum permeation of model solutes. *J. Pharm. Sci.* **2003**, *92*, 344–359. [[CrossRef](#)] [[PubMed](#)]
34. Nielsen, H.M.; Rassing, M.R. TR146 cells grown on filters as a model of human buccal epithelium: IV. Permeability of water, mannitol, testosterone and beta-adrenoceptor antagonists. Comparison to human, monkey and porcine buccal mucosa. *Int. J. Pharm.* **2000**, *194*, 155–167. [[CrossRef](#)]
35. Shojaei, A.H.; Berner, B.; Xiaoling, L. Transbuccal delivery of acyclovir: I. In vitro determination of routes of buccal transport. *Pharm. Res.* **1998**, *15*, 1182–1188. [[CrossRef](#)] [[PubMed](#)]
36. Shojaei, A.H.; Zhuo, S.L.; Li, X. Transbuccal delivery of acyclovir (II): Feasibility, system design, and in vitro permeation studies. *J. Pharm. Pharm. Sci.* **1998**, *1*, 66–73.
37. Kulkarni, U.; Mahalingam, R.; Pather, S.I.; Li, X.; Jasti, B. Porcine buccal mucosa as an in vitro model: Relative contribution of epithelium and connective tissue as permeability barriers. *J. Pharm. Sci.* **2009**, *98*, 471–483. [[CrossRef](#)] [[PubMed](#)]

38. Jacobsen, J. Buccal iontophoretic delivery of atenolol-HCl employing a new in vitro three-chamber permeation cell. *J. Control. Release* **2001**, *70*, 83–95. [[CrossRef](#)]
39. Atlabachew, M.; Combrinck, S.; Viljoen, A.M.; Hamman, J.H.; Gouws, C. Isolation and in vitro permeation of phenylpropylamino alkaloids from Khat (*Catha edulis*) across oral and intestinal mucosal tissues. *J. Ethnopharmacol.* **2016**, *194*, 307–315. [[CrossRef](#)] [[PubMed](#)]
40. Adhikari, S.N.R.; Panda, S. Buccal patches of atenolol formulated using fenugreek (*Trigonella foenum-graecum* L.) seed mucilage. *Polim. Med.* **2017**, *47*, 5–11. [[CrossRef](#)]
41. Amaral, B.R.; Argenta, D.F.; Kroth, R.; Caon, T. Transbuccal delivery of benznidazole associated with monoterpenes: Permeation studies and mechanistic insights. *Eur. J. Pharm. Sci.* **2020**, *143*, 105177. [[CrossRef](#)] [[PubMed](#)]
42. Birudaraj, R.; Berner, B.; Shen, S.; Li, X. Buccal permeation of buspirone: Mechanistic studies on transport pathways. *J. Pharm. Sci.* **2005**, *94*, 70–78. [[CrossRef](#)] [[PubMed](#)]
43. Nicolazzo, J.A.; Reed, B.L.; Finnin, B.C. Modification of buccal drug delivery following pretreatment with skin penetration enhancers. *J. Pharm. Sci.* **2004**, *93*, 2054–2063. [[CrossRef](#)]
44. Nicolazzo, J.A.; Reed, B.L.; Finnin, B.C. The effect of various in vitro conditions on the permeability characteristics of the buccal mucosa. *J. Pharm. Sci.* **2003**, *92*, 2399–2410. [[CrossRef](#)] [[PubMed](#)]
45. Hansen, S.E.; Marxen, E.; Janfelt, C.; Jacobsen, J. Buccal delivery of small molecules—Impact of levulinic acid, oleic acid, sodium dodecyl sulfate and hypotonicity on ex vivo permeability and spatial distribution in mucosa. *Eur. J. Pharm. Biopharm.* **2018**, *133*, 250–257. [[CrossRef](#)] [[PubMed](#)]
46. Caon, T.; Simoes, C.M. Effect of freezing and type of mucosa on ex vivo drug permeability parameters. *AAPS PharmSciTech* **2011**, *12*, 587–592. [[CrossRef](#)]
47. Gomez-Segura, L.; Parra, A.; Calpena, A.C.; Gimeno, A.; Boix-Montanes, A. Carprofen permeation test through porcine ex vivo mucous membranes and ophthalmic tissues for tolerability assessments: Validation and histological study. *Vet. Sci.* **2020**, *7*, 152. [[CrossRef](#)]
48. Yamsani, V.V.; Gannu, R.; Kolli, C.; Rao, M.E.; Yamsani, M.R. Development and in vitro evaluation of buccoadhesive carvedilol tablets. *Acta Pharm.* **2007**, *57*, 185–197. [[CrossRef](#)]
49. Chen, J.; Duan, H.; Pan, H.; Yang, X.; Pan, W. Two types of core/shell fibers based on carboxymethyl chitosan and Sodium carboxymethyl cellulose with self-assembled liposome for buccal delivery of carvedilol across TR146 cell culture and porcine buccal mucosa. *Int. J. Biol. Macromol.* **2019**, *128*, 700–709. [[CrossRef](#)]
50. Vishnu, Y.V.; Chandrasekhar, K.; Ramesh, G.; Rao, Y.M. Development of mucoadhesive patches for buccal administration of carvedilol. *Curr. Drug Deliv.* **2007**, *4*, 27–39. [[CrossRef](#)]
51. Mahalingam, R.; Ravivarapu, H.; Redkar, S.; Li, X.; Jasti, B.R. Transbuccal delivery of 5-aza-2'-deoxycytidine: Effects of drug concentration, buffer solution, and bile salts on permeation. *AAPS PharmSciTech* **2007**, *8*, E28–E33. [[CrossRef](#)] [[PubMed](#)]
52. Marxen, E.; Axelsen, M.C.; Pedersen, A.M.L.; Jacobsen, J. Effect of cryoprotectants for maintaining drug permeability barriers in porcine buccal mucosa. *Int. J. Pharm.* **2016**, *511*, 599–605. [[CrossRef](#)]
53. Ojewole, E.; Mackraj, I.; Akhundov, K.; Hamman, J.; Viljoen, A.; Olivier, E.; Wesley-Smith, J.; Govender, T. Investigating the effect of Aloe vera gel on the buccal permeability of didanosine. *Planta Med.* **2012**, *78*, 354–361. [[CrossRef](#)]
54. Rambharose, S.; Ojewole, E.; Mackraj, I.; Govender, T. Comparative buccal permeability enhancement of didanosine and tenofovir by potential multifunctional polymeric excipients and their effects on porcine buccal histology. *Pharm. Dev. Technol.* **2014**, *19*, 82–90. [[CrossRef](#)]
55. Ojewole, E.; Kalthapure, R.; Akamanchi, K.; Govender, T. Novel oleic acid derivatives enhance buccal permeation of didanosine. *Drug Dev. Ind. Pharm.* **2014**, *40*, 657–668. [[CrossRef](#)] [[PubMed](#)]
56. Shojaei, A.H.; Khan, M.; Lim, G.; Khosravan, R. Transbuccal permeation of a nucleoside analog, dideoxycytidine: Effects of menthol as a permeation enhancer. *Int. J. Pharm.* **1999**, *192*, 139–146. [[CrossRef](#)]
57. Xiang, J.; Fang, X.; Li, X. Transbuccal delivery of 2',3'-dideoxycytidine: In vitro permeation study and histological investigation. *Int. J. Pharm.* **2002**, *231*, 57–66. [[CrossRef](#)]
58. Hu, L.; Silva, S.M.; Damaj, B.B.; Martin, R.; Michniak-Kohn, B.B. Transdermal and transbuccal drug delivery systems: Enhancement using iontophoretic and chemical approaches. *Int. J. Pharm.* **2011**, *421*, 53–62. [[CrossRef](#)]
59. Caon, T.; Pan, Y.; Simoes, C.M.; Nicolazzo, J.A. Exploiting the buccal mucosa as an alternative route for the delivery of donepezil hydrochloride. *J. Pharm. Sci.* **2014**, *103*, 1643–1651. [[CrossRef](#)]
60. Gimeno, A.; Calpena, A.C.; Sanz, R.; Mallandrich, M.; Paire, C.; Clares, B. Transbuccal delivery of doxepin: Studies on permeation and histological investigation. *Int. J. Pharm.* **2014**, *477*, 650–654. [[CrossRef](#)]
61. Bird, A.P.; Faltinek, J.R.; Shojaei, A.H. Transbuccal peptide delivery: Stability and in vitro permeation studies on endomorphin-1. *J. Control. Release* **2001**, *73*, 31–36. [[CrossRef](#)]
62. Nicolazzo, J.A.; Reed, B.L.; Finnin, B.C. Enhanced buccal mucosal retention and reduced buccal permeability of estradiol in the presence of padimate O and Azone: A mechanistic study. *J. Pharm. Sci.* **2005**, *94*, 873–882. [[CrossRef](#)] [[PubMed](#)]
63. Palem, C.R.; Gannu, R.; Yamsani, S.K.; Yamsani, V.V.; Yamsani, M.R. Development of bioadhesive buccal tablets for felodipine and pioglitazone in combined dosage form: In vitro, ex vivo, and in vivo characterization. *Drug Deliv.* **2011**, *18*, 344–352. [[CrossRef](#)] [[PubMed](#)]

64. Diaz Del Consuelo, I.; Pizzolato, G.P.; Falson, F.; Guy, R.H.; Jacques, Y. Evaluation of pig esophageal mucosa as a permeability barrier model for buccal tissue. *J. Pharm. Sci.* **2005**, *94*, 2777–2788. [[CrossRef](#)] [[PubMed](#)]
65. Hoogstraate, A.J.; Cullander, C.; Nagelkerke, J.F.; Senel, S.; Verhoef, J.C.; Junginger, H.E.; Bodde, H.E. Diffusion rates and transport pathways of fluorescein isothiocyanate (FITC)-labeled model compounds through buccal epithelium. *Pharm. Res.* **1994**, *11*, 83–89. [[CrossRef](#)] [[PubMed](#)]
66. Sandri, G.; Rossi, S.; Bonferoni, M.C.; Ferrari, F.; Zambito, Y.; Di Colo, G.; Caramella, C. Buccal penetration enhancement properties of N-trimethyl chitosan: Influence of quaternization degree on absorption of a high molecular weight molecule. *Int. J. Pharm.* **2005**, *297*, 146–155. [[CrossRef](#)]
67. Deneer, V.H.; Drese, G.B.; Roemele, P.E.; Verhoef, J.C.; Lie, A.H.L.; Kingma, J.H.; Brouwers, J.R.; Junginger, H.E. Buccal transport of flecainide and sotalol: Effect of a bile salt and ionization state. *Int. J. Pharm.* **2002**, *241*, 127–134. [[CrossRef](#)]
68. De Caro, V.; Giandalia, G.; Siragusa, M.G.; Paderni, C.; Campisi, G.; Giannola, L.I. Evaluation of galantamine transbuccal absorption by reconstituted human oral epithelium and porcine tissue as buccal mucosa models: Part I. *Eur. J. Pharm. Biopharm.* **2008**, *70*, 869–873. [[CrossRef](#)] [[PubMed](#)]
69. Ceschel, G.C.; Maffei, P.; Lombardi Borgia, S.; Ronchi, C. Design and evaluation of buccal adhesive hydrocortisone acetate (HCA) tablets. *Drug Deliv.* **2001**, *8*, 161–171. [[CrossRef](#)] [[PubMed](#)]
70. Bashyal, S.; Seo, J.E.; Keum, T.; Noh, G.; Lamichhane, S.; Kim, J.H.; Kim, C.H.; Choi, Y.W.; Lee, S. Facilitated buccal insulin delivery via hydrophobic ion-pairing approach: In vitro and ex vivo evaluation. *Int. J. Nanomed.* **2021**, *16*, 4677–4691. [[CrossRef](#)]
71. Shah, V.; Bellantone, R.A.; Taft, D.R. Evaluating the potential for delivery of irinotecan via the buccal route: Physicochemical characterization and in vitro permeation assessment across porcine buccal mucosa. *AAPS PharmSciTech* **2017**, *18*, 867–874. [[CrossRef](#)]
72. Kroth, R.; Argenta, D.F.; Conte, J.; Amaral, B.R.; Caon, T. Transbuccal delivery of isoniazid: Ex vivo permeability and drug-surfactant interaction studies. *AAPS PharmSciTech* **2020**, *21*, 289. [[CrossRef](#)] [[PubMed](#)]
73. Eleftheriadis, G.K.; Monou, P.K.; Bouropoulos, N.; Boetker, J.; Rantanen, J.; Jacobsen, J.; Vizirianakis, I.S.; Fatouros, D.G. Fabrication of mucoadhesive buccal films for local administration of ketoprofen and lidocaine hydrochloride by combining fused deposition modeling and inkjet printing. *J. Pharm. Sci.* **2020**, *109*, 2757–2766. [[CrossRef](#)] [[PubMed](#)]
74. Mashru, R.; Sutariya, V.; Sankalia, M.; Sankalia, J. Transbuccal delivery of lamotrigine across porcine buccal mucosa: In vitro determination of routes of buccal transport. *J. Pharm. Pharm. Sci.* **2005**, *8*, 54–62.
75. Franz-Montan, M.; Serpe, L.; Martinelli, C.C.; da Silva, C.B.; Santos, C.P.; Novaes, P.D.; Volpato, M.C.; de Paula, E.; Lopez, R.F.; Groppo, F.C. Evaluation of different pig oral mucosa sites as permeability barrier models for drug permeation studies. *Eur. J. Pharm. Sci.* **2016**, *81*, 52–59. [[CrossRef](#)] [[PubMed](#)]
76. do Couto, R.O.; Cubayachi, C.; Calefi, P.L.; Lopez, R.F.V.; Pedrazzi, V.; De Gaitani, C.M.; de Freitas, O. Combining amino amide salts in mucoadhesive films enhances needle-free buccal anesthesia in adults. *J. Control. Release* **2017**, *266*, 205–215. [[CrossRef](#)]
77. Abu-Huwajj, R.; Assaf, S.; Salem, M.; Sallam, A. Potential mucoadhesive dosage form of lidocaine hydrochloride: II. In vitro and in vivo evaluation. *Drug Dev. Ind. Pharm.* **2007**, *33*, 437–448. [[CrossRef](#)] [[PubMed](#)]
78. Meng-Lund, E.; Marxen, E.; Pedersen, A.M.L.; Mullertz, A.; Hyrup, B.; Holm, R.; Jacobsen, J. Ex vivo correlation of the permeability of metoprolol across human and porcine buccal mucosa. *J. Pharm. Sci.* **2014**, *103*, 2053–2061. [[CrossRef](#)]
79. Marxen, E.; Mosgaard, M.D.; Pedersen, A.M.L.; Jacobsen, J. Mucin dispersions as a model for the oromucosal mucus layer in in vitro and ex vivo buccal permeability studies of small molecules. *Eur. J. Pharm. Biopharm.* **2017**, *121*, 121–128. [[CrossRef](#)]
80. Marxen, E.; Jin, L.; Jacobsen, J.; Janfelt, C.; Hyrup, B.; Nicolazzo, J.A. Effect of permeation enhancers on the buccal permeability of nicotine: Ex vivo transport studies complemented by MALDI MS imaging. *Pharm. Res.* **2018**, *35*, 70. [[CrossRef](#)] [[PubMed](#)]
81. Lee, J.; Lee, S.K.; Choi, Y.W. The effect of storage conditions on the permeability of porcine buccal mucosa. *Arch. Pharm. Res.* **2002**, *25*, 546–549. [[CrossRef](#)] [[PubMed](#)]
82. Holm, R.; Meng-Lund, E.; Andersen, M.B.; Jespersen, M.L.; Karlsson, J.J.; Garmer, M.; Jorgensen, E.B.; Jacobsen, J. In vitro, ex vivo and in vivo examination of buccal absorption of metoprolol with varying pH in TR146 cell culture, porcine buccal mucosa and Gottingen minipigs. *Eur. J. Pharm. Sci.* **2013**, *49*, 117–124. [[CrossRef](#)] [[PubMed](#)]
83. Senel, S.; Duchene, D.; Hincal, A.A.; Capan, Y.; Ponchel, G. In vitro studies on enhancing effect of sodium glycocholate on transbuccal permeation of morphine hydrochloride. *J. Control. Release* **1998**, *51*, 107–113. [[CrossRef](#)] [[PubMed](#)]
84. Senel, S.; Hincal, A.A. Drug permeation enhancement via buccal route: Possibilities and limitations. *J. Control. Release* **2001**, *72*, 133–144. [[CrossRef](#)]
85. Giannola, L.I.; De Caro, V.; Giandalia, G.; Siragusa, M.G.; Tripodo, C.; Florena, A.M.; Campisi, G. Release of naltrexone on buccal mucosa: Permeation studies, histological aspects and matrix system design. *Eur. J. Pharm. Biopharm.* **2007**, *67*, 425–433. [[CrossRef](#)]
86. Rai, V.; Tan, H.S.; Michniak-Kohn, B. Effect of surfactants and pH on naltrexone (NTX) permeation across buccal mucosa. *Int. J. Pharm.* **2011**, *411*, 92–97. [[CrossRef](#)]
87. Nair, M.K.; Chetty, D.J.; Ho, H.; Chien, Y.W. Biomembrane permeation of nicotine: Mechanistic studies with porcine mucosae and skin. *J. Pharm. Sci.* **1997**, *86*, 257–262. [[CrossRef](#)] [[PubMed](#)]
88. Chen, L.L.; Chetty, D.J.; Chien, Y.W. A mechanistic analysis to characterize oramucosal permeation properties. *Int. J. Pharm.* **1999**, *184*, 63–72. [[CrossRef](#)]
89. Nielsen, H.M.; Rassing, M.R. Nicotine permeability across the buccal TR146 cell culture model and porcine buccal mucosa in vitro: Effect of pH and concentration. *Eur. J. Pharm. Sci.* **2002**, *16*, 151–157. [[CrossRef](#)]

90. Marxen, E.; Jacobsen, J.; Hyrup, B.; Janfelt, C. Permeability barriers for nicotine and mannitol in porcine buccal mucosa studied by high-resolution MALDI mass spectrometry imaging. *Mol. Pharm.* **2018**, *15*, 519–526. [[CrossRef](#)] [[PubMed](#)]
91. Jasti, B.R.; Zhou, S.; Mehta, R.C.; Li, X. Permeability of antisense oligonucleotide through porcine buccal mucosa. *Int. J. Pharm.* **2000**, *208*, 35–39. [[CrossRef](#)]
92. Figueiras, A.; Hombach, J.; Veiga, F.; Bernkop-Schnurch, A. In vitro evaluation of natural and methylated cyclodextrins as buccal permeation enhancing system for omeprazole delivery. *Eur. J. Pharm. Biopharm.* **2009**, *71*, 339–345. [[CrossRef](#)] [[PubMed](#)]
93. Mashru, R.C.; Sutariya, V.B.; Sankalia, M.G.; Sankalia, J.M. Effect of pH on in vitro permeation of ondansetron hydrochloride across porcine buccal mucosa. *Pharm. Dev. Technol.* **2005**, *10*, 241–247. [[CrossRef](#)] [[PubMed](#)]
94. Hu, L.; Damaj, B.B.; Martin, R.; Michniak-Kohn, B.B. Enhanced in vitro transbuccal drug delivery of ondansetron HCl. *Int. J. Pharm.* **2011**, *404*, 66–74. [[CrossRef](#)]
95. Silva-Abreu, M.; Espinoza, L.C.; Halbaut, L.; Espina, M.; Garcia, M.L.; Calpena, A.C. Comparative study of ex vivo transmucosal permeation of pioglitazone nanoparticles for the treatment of Alzheimer's disease. *Polymers* **2018**, *10*, 316. [[CrossRef](#)] [[PubMed](#)]
96. Goswami, T.; Jasti, B.R.; Li, X. Estimation of the theoretical pore sizes of the porcine oral mucosa for permeation of hydrophilic permeants. *Arch. Oral Biol.* **2009**, *54*, 577–582. [[CrossRef](#)] [[PubMed](#)]
97. Amores, S.; Domenech, J.; Colom, H.; Calpena, A.C.; Clares, B.; Gimeno, A.; Lauroba, J. An improved cryopreservation method for porcine buccal mucosa in ex vivo drug permeation studies using Franz diffusion cells. *Eur. J. Pharm. Sci.* **2014**, *60*, 49–54. [[CrossRef](#)]
98. Prasanth, V.V.; Puratchikody, A.; Mathew, S.T.; Ashok, K.B. Effect of permeation enhancers in the mucoadhesive buccal patches of salbutamol sulphate for unidirectional buccal drug delivery. *Res. Pharm. Sci.* **2014**, *9*, 259–268.
99. Oh, D.H.; Chun, K.H.; Jeon, S.O.; Kang, J.W.; Lee, S. Enhanced transbuccal salmon calcitonin (sCT) delivery: Effect of chemical enhancers and electrical assistance on in vitro sCT buccal permeation. *Eur. J. Pharm. Biopharm.* **2011**, *79*, 357–363. [[CrossRef](#)]
100. Keum, T.; Noh, G.; Seo, J.E.; Bashyal, S.; Lee, S. In vitro and ex vivo evaluation of penetratin as a non-invasive permeation enhancer in the penetration of salmon calcitonin through TR146 buccal cells and porcine buccal tissues. *Pharmaceutics* **2020**, *13*, 408. [[CrossRef](#)]
101. Rambharose, S.; Ojewole, E.; Branham, M.; Kalhapure, R.; Govender, T. High-energy ball milling of saquinavir increases permeability across the buccal mucosa. *Drug Dev. Ind. Pharm.* **2014**, *40*, 639–648. [[CrossRef](#)]
102. Vermaak, I.; Viljoen, A.M.; Chen, W.; Hamman, J.H. In vitro transport of the steroidal glycoside P57 from Hoodia gordonii across excised porcine intestinal and buccal tissue. *Phytomedicine* **2011**, *18*, 783–787. [[CrossRef](#)]
103. Gore, A.V.; Liang, A.C.; Chien, Y.W. Comparative biomembrane permeation of tacrine using Yucatan minipigs and domestic pigs as the animal model. *J. Pharm. Sci.* **1998**, *87*, 441–447. [[CrossRef](#)] [[PubMed](#)]
104. Liu, C.; Xu, H.N.; Li, X.L. In vitro permeation of tetramethylpyrazine across porcine buccal mucosa. *Acta Pharmacol. Sin.* **2002**, *23*, 792–796. [[PubMed](#)]
105. Artusi, M.; Santi, P.; Colombo, P.; Junginger, H.E. Buccal delivery of thiocolchicoside: In vitro and in vivo permeation studies. *Int. J. Pharm.* **2003**, *250*, 203–213. [[CrossRef](#)]
106. Shin, S.C.; Kim, J.Y. Enhanced permeation of triamcinolone acetonide through the buccal mucosa. *Eur. J. Pharm. Biopharm.* **2000**, *50*, 217–220. [[CrossRef](#)]
107. Nicolazzo, J.A.; Reed, B.L.; Finnin, B.C. Enhancing the buccal mucosal uptake and retention of triamcinolone acetonide. *J. Control. Release* **2005**, *105*, 240–248. [[CrossRef](#)] [[PubMed](#)]
108. NIH. PubChem. Available online: <https://pubchem.ncbi.nlm.nih.gov/> (accessed on 19 September 2021).
109. Tsutsumi, K.; Obata, Y.; Takayama, K.; Isowa, K.; Nagai, T. Permeation of several drugs through keratinized epithelial-free membrane of hamster cheek pouch. *Int. J. Pharm.* **1999**, *177*, 7–14. [[CrossRef](#)]
110. Koschier, F.; Kostrubsky, V.; Toole, C.; Gallo, M.A. In vitro effects of ethanol and mouthrinse on permeability in an oral buccal mucosal tissue construct. *Food Chem. Toxicol.* **2011**, *49*, 2524–2529. [[CrossRef](#)]
111. Galey, W.R.; Lonsdale, H.K.; Nacht, S. The in vitro permeability of skin and buccal mucosa to selected drugs and tritiated water. *J. Investig. Dermatol.* **1976**, *67*, 713–717. [[CrossRef](#)] [[PubMed](#)]
112. Streisand, J.B.; Zhang, J.; Niu, S.; McJames, S.; Natte, R.; Pace, N.L. Buccal absorption of fentanyl is pH-dependent in dogs. *Anesthesiology* **1995**, *82*, 759–764. [[CrossRef](#)] [[PubMed](#)]
113. Xue, X.Y.; Zhou, Y.; Chen, Y.Y.; Meng, J.R.; Jia, M.; Hou, Z.; Bai, H.; Mao, X.G.; Luo, X.X. Promoting effects of chemical permeation enhancers on insulin permeation across TR146 cell model of buccal epithelium in vitro. *Drug Chem. Toxicol.* **2012**, *35*, 199–207. [[CrossRef](#)] [[PubMed](#)]
114. Jacobsen, J.; Nielsen, E.B.; Brondum-Nielsen, K.; Christensen, M.E.; Olin, H.B.; Tommerup, N.; Rassing, M.R. Filter-grown TR146 cells as an in vitro model of human buccal epithelial permeability. *Eur. J. Oral Sci.* **1999**, *107*, 138–146. [[CrossRef](#)] [[PubMed](#)]
115. Giannola, L.I.; De Caro, V.; Giandalia, G.; Siragusa, M.G.; Campisi, G.; Florena, A.M.; Ciach, T. Diffusion of naltrexone across reconstituted human oral epithelium and histomorphological features. *Eur. J. Pharm. Biopharm.* **2007**, *65*, 238–246. [[CrossRef](#)]
116. Adrian, C.L.; Olin, H.B.; Dalhoff, K.; Jacobsen, J. In vivo human buccal permeability of nicotine. *Int. J. Pharm.* **2006**, *311*, 196–202. [[CrossRef](#)] [[PubMed](#)]
117. Mehta, M.; Kempainen, B.W.; Stafford, R.G. In vitro penetration of tritium-labelled water (THO) and [³H]PbTx-3 (a red tide toxin) through monkey buccal mucosa and skin. *Toxicol. Lett.* **1991**, *55*, 185–194. [[CrossRef](#)]
118. Squier, C.A. The permeability of oral mucosa. *Crit. Rev. Oral Biol. Med.* **1991**, *2*, 13–32. [[CrossRef](#)] [[PubMed](#)]

119. Chilcott, R.P.; Barai, N.; Beezer, A.E.; Brain, S.I.; Brown, M.B.; Bunge, A.L.; Burgess, S.E.; Cross, S.; Dalton, C.H.; Dias, M.; et al. Inter- and intralaboratory variation of in vitro diffusion cell measurements: An international multicenter study using quasi-standardized methods and materials. *J. Pharm. Sci.* **2005**, *94*, 632–638. [[CrossRef](#)] [[PubMed](#)]
120. Ho, N.F.H.; Raub, T.J.; Burton, P.S.; Barsuhn, C.L.; Adson, A.; Audus, K.L.; Borchardt, R.T. Quantitative approaches to delineate passive transport mechanisms in cell culture monolayers. In *Transport Processes in Pharmaceutical Systems*; Amidon, G., Lee, P., Topp, E., Eds.; CRC Press: Boca Raton, FL, USA, 1999; pp. 219–316.
121. Kim, Y.H.; Ghanem, A.H.; Higuchi, W.I. Model studies of epidermal permeability. *Semin. Dermatol.* **1992**, *11*, 145–156. [[PubMed](#)]
122. Xiang, T.; Xu, Y.; Anderson, B.D. The barrier domain for solute permeation varies with lipid bilayer phase structure. *J. Membr. Biol.* **1998**, *165*, 77–90. [[CrossRef](#)]
123. Li, S.K.; Hao, J. Transscleral passive and iontophoretic transport: Theory and analysis. *Expert Opin. Drug Deliv.* **2018**, *15*, 283–299. [[CrossRef](#)]
124. Adson, A.; Raub, T.J.; Burton, P.S.; Barsuhn, C.L.; Hilgers, A.R.; Audus, K.L.; Ho, N.F. Quantitative approaches to delineate paracellular diffusion in cultured epithelial cell monolayers. *J. Pharm. Sci.* **1994**, *83*, 1529–1536. [[CrossRef](#)] [[PubMed](#)]
125. Deen, W.M. Hindered transport of large molecules in liquid-filled pores. *AIChE* **1987**, *33*, 1409–1425. [[CrossRef](#)]
126. Hao, J.; Li, S.K. Transungual iontophoretic transport of polar neutral and positively charged model permeants: Effects of electrophoresis and electroosmosis. *J. Pharm. Sci.* **2008**, *97*, 893–905. [[CrossRef](#)] [[PubMed](#)]
127. Ren, W.; Baig, A.; Li, S.K. Passive and iontophoretic transport of fluorides across enamel in vitro. *J. Pharm. Sci.* **2014**, *103*, 1692–1700. [[CrossRef](#)] [[PubMed](#)]
128. Wen, H.; Hao, J.; Li, S.K. Characterization of human sclera barrier properties for transscleral delivery of bevacizumab and ranibizumab. *J. Pharm. Sci.* **2013**, *102*, 892–903. [[CrossRef](#)] [[PubMed](#)]
129. Chantasart, D.; Chootanasoontorn, S.; Suksiriworapong, J.; Li, S.K. Investigation of pH influence on skin permeation behavior of weak acids using nonsteroidal anti-inflammatory drugs. *J. Pharm. Sci.* **2015**, *104*, 3459–3470. [[CrossRef](#)]
130. Fleisher, D. Biological Transport Phenomena in the Gastrointestinal Tract: Cellular Mechanisms. In *Transport Processes in Pharmaceutical Systems*, 1st ed.; Amidon, G.L., Lee, P.I., Topp, E.M., Eds.; CRC Press: Boca Raton, FL, USA, 1999.
131. Winne, D. Shift of pH-absorption curves. *J. Pharmacokinet. Biopharm.* **1977**, *5*, 53–94. [[CrossRef](#)] [[PubMed](#)]
132. Prausnitz, M.R.; Noonan, J.S. Permeability of cornea, sclera, and conjunctiva: A literature analysis for drug delivery to the eye. *J. Pharm. Sci.* **1998**, *87*, 1479–1488. [[CrossRef](#)]
133. Li, S.K.; Peck, K.D. Passive and iontophoretic transport through the skin polar pathway. *Skin Pharmacol. Physiol.* **2013**, *26*, 243–253. [[CrossRef](#)]
134. Hamalainen, K.M.; Kananen, K.; Auriola, S.; Kontturi, K.; Urtti, A. Characterization of paracellular and aqueous penetration routes in cornea, conjunctiva, and sclera. *Investig. Ophthalmol. Vis. Sci.* **1997**, *38*, 627–634.